

Worcester Polytechnic Institute Digital WPI

Major Qualifying Projects (All Years)

Major Qualifying Projects

June 2016

Biological Models With Time Delay

Nonthakorn Olanant

Worcester Polytechnic Institute

Xinyang Guan

Worcester Polytechnic Institute

Follow this and additional works at: <https://digitalcommons.wpi.edu/mqp-all>

Repository Citation

Olanant, N., & Guan, X. (2016). *Biological Models With Time Delay*. Retrieved from <https://digitalcommons.wpi.edu/mqp-all/3166>

This Unrestricted is brought to you for free and open access by the Major Qualifying Projects at Digital WPI. It has been accepted for inclusion in Major Qualifying Projects (All Years) by an authorized administrator of Digital WPI. For more information, please contact digitalwpi@wpi.edu.

Project Number: MA-RYL-2016

Biological Models With Time Delay

A Major Qualifying Project

submitted to the Faculty

of the

WORCESTER POLYTECHNIC INSTITUTE

in partial fulfillment of the requirements for the

Degree of Bachelor of Science

by

Olaranont Nonthakorn

Xinyang Guan

June 28, 2016

Approved

Professor Roger Y. Lui
Major Advisor

Abstract

This Major Qualifying Project can be divided into three main chapters. For each chapter, we studied three different mathematical models, which are the Logistic Growth model, the SIR model and the Chemostat model. These biological mathematical models all have time delay in part of their processes. Based on the specific phenomenological assumptions, we have different ways of building up the model through ordinary differential equations. In this way, we can push the basic model into a more realistic level. The goal of this project is to investigate three models with time delay. Specifically to perform phase plane analysis and find the concept of Basic Reproduction Number (denoted by R_0) for SIR model with time delay. We will also perform global sensitivity analysis for each model and study how uncertainty in the output of each model can be attributed to different sources of uncertainty in the model input. Applications for each model with time delay will be provided in this project with numerical results.

Acknowledgement

We would like to thank Professor Roger Lui of the Mathematical Sciences Department for his continuous advice and assistance throughout this project. We would also like to thank Heng Zuo of the Mathematics Sciences Department, who assisted us in building the global sensitivity analysis model.

Contents

1	Introduction	7
1.1	Logistic Growth	7
1.2	SIR model	8
1.2.1	Incubation Period	9
1.2.2	Loss of Immunity	10
1.3	Chemostat model	11
2	Steady-states and Characteristic Equations	14
2.1	Logistic growth model with delay	15
2.1.1	Steady-states	15
2.1.2	Characteristic equation	15
2.2	SEIR model with delay	16
2.2.1	Steady-states	16
2.2.2	Characteristic equation	17
2.3	SIRS model with delay	19
2.3.1	Steady-states	19
2.3.2	Characteristic equation	21
2.4	Chemostat model with delay	22
2.4.1	Steady-states	23
2.4.2	Characteristic equation	23
3	Stability Analysis	26
3.1	Logistic growth model with delay	27
3.2	SEIR model with delay	29
3.2.1	Steady-state E_1	29
3.2.2	Steady-state E_2	30
3.3	SIRS model with delay	31
3.3.1	Steady-state E_3	31
3.3.2	Steady-state E_4	35
3.4	Chemostat model with delay	39
3.4.1	Steady-state F_1	39
3.4.2	Steady-state F_2	40

4	Global Sensitivity Analysis	42
4.1	The SEIR model with Incubation Period	44
4.1.1	Global Sensitivity Analysis with Peak of $I(t)$	46
4.1.2	Global Sensitivity Analysis with $t(I)$	47
4.1.3	Global Sensitivity Analysis with $\int_0^T I(t)dt$	48
4.2	The Chemostat	49
4.2.1	Global Sensitivity Analysis with $\int_0^T X(t)dt$	50
5	Conclusion	51
	Appendix A MATLAB Code	52

List of Tables

1.1	Introduce the variables and parameters of chemostat model	13
4.1	Parameters of interest(POI) for the SEIR Model	44
4.2	Quantities of interest(QOI) for the SEIR Model	44
4.3	Fixed parameters for the SEIR Model	45
4.4	Parameters of interest(POI) for the Chemostat Model	49
4.5	Quantities of interest(QOI) for the Chemostat Model	49

List of Figures

1.1	Schematic diagram for the SIR model	9
1.2	A scheme of chemostat [1]	11
1.3	Michealis-Menten Kinetic, S in the picture is the same as N in the chemostat model, $Vmax$ represents K_1 , and Km represents K_2	13
3.1	$\tau = \frac{\pi}{4} + 0.1$	28
3.2	$\tau = \frac{\pi}{4} - 0.1$	28
3.3	$\omega_1 > \omega^*$	33
3.4	$\omega_1 = 80\%$ of ω^*	34
3.5	$\omega_1 = 70\%$ of ω^*	34
3.6	$\omega_1 = 60\%$ of ω^*	35
3.7	$\omega = \omega^*$	37
3.8	$\omega = \omega^* - 0.1$	37
3.9	$\omega = \omega^* + 0.1$	37
3.10	$\omega = \omega^* + 0.2$	37
3.11	$\omega = \omega^* + 0.3$	37
3.12	$R_0 = 1.6346$	38
3.13	$R_0 = 2.8302$	38
3.14	$R_0 = 2.8846$	38
3.15	$R_0 = 3.7037$	38
4.1	The Process of Global Sensitivity Analysis	42
4.2	$Peak - I(t) - \beta \in (0.4, 2), \gamma = 1/6, \tau = 5, h = 50$	46
4.3	$Peak - I(t) - \gamma \in (1/2, 1/7), \beta = 1, \tau = 5, h = 400$	46
4.4	$Peak - I(t) - \tau \in (0, 10), \gamma = 1/6, \beta = 1, h = 50$	46
4.5	$t(I) - \beta \in (0.4, 2), \gamma = 1/4, \tau = 5$	47
4.6	$t(I) - \gamma \in (1/2, 1/7), \beta = 1, \tau = 5$	47
4.7	$t(I) - \tau \in (0, 10), \beta = 1, \gamma = 1/4$	47
4.8	$\int_0^T I(t)dt - \beta \in (0.4, 2), \gamma = 1/4, \tau = 5, h = 1000$	48
4.9	$\int_0^T I(t)dt - \gamma \in (1/2, 1/7), \beta = 1, \tau = 5, h = 1000$	48
4.10	$\int_0^T I(t)dt - \tau \in (0, 10), \gamma = 1/4, \beta = 1, h = 1000$	48
4.11	$\int_0^T X(t)dt - K_1 \in (0.1, 1), K_2 = 0.0727, \omega = 1.1$	50
4.12	$\int_0^T X(t)dt - K_2 \in (0.01, 0.1), K_1 = 0.7726, \omega = 1.1$	50
4.13	$\int_0^T X(t)dt - \omega \in (0.1, 1.2), K_1 = 0.7726, K_2 = 0.0727$	50

Chapter 1

Introduction

Communicable diseases such as measles, tuberculosis are a fact of our life. Some diseases are not directly transmitted from human to human but transmitted by agents such as mosquito or tick.

Many mathematical models are developed for building the numerical relationships between the vectors and the hosts. The compartmental models in epidemiology are popularly used for modeling the establishment and spread of infectious diseases. By modeling the main characteristics of the system, the compartmental model, as a basic mathematical framework, contributes to explaining the complex phenomenon between pathogen and hosts.

Based on the specific phenomenological assumptions, we have different ways of building up the model using ordinary differential equations. Many classical epidemic models have been studied and published, such as SIR, SIS and SEIR. Delay differential equation is one of the most popular areas in this particular biological science. We study many examples of delay differential equations which can be found in [2]. By contrast with ordinary differential equations, delay equations use the solution from the priors time into the next derivative at every time. The simple constant delay time can be formed in the following equation

$$\frac{dy(t)}{dt} = f(t, y(t), y(t - \tau_1), y(t - \tau_2), \dots, y(t - \tau_k)) \quad (1.1)$$

where the time delays (lags) τ_j are positive constants. For more explanations of how ordinary differential equations transform to delay differential equations, please see in [3].

1.1 Logistic Growth

The logistic equation is a model of population growth first published by Pierre Verhulst (1845, 1847) for modeling the reality of limited resources. This model is continuous in time, but a modification of the continuous equation to a discrete quadratic recurrence equation known as the logistic map is also widely used.

The continuous version of the logistic model is described by the differential equation

$$\frac{dN}{dt} = \frac{rN(K - N)}{K} \quad (1.2)$$

where r is the Malthusian parameter (rate of maximum population growth) and K is the carrying capacity. Dividing both sides by K and defining $x = N/K$ then gives the differential equation

$$\frac{dx}{dt} = rx(1 - x) \quad (1.3)$$

The logisitc equation assumes that the organisms birth rate depends instantaneously on changes in population size. However, in many cases, there should be a delay. For example, many organisms store nutrients, so people wont notice immediately if the population grows too large for the available resourses. In 1948 G. E. Hutchinson modified the logistic equation to incorporate a delay into the growth rate. So the model becomes

$$\frac{dN}{dt} = rN[1 - \frac{N(t - \tau)}{K}] \quad (1.4)$$

where the τ is time delay.

1.2 SIR model

SIR model, the basic epidemic model, yields a relatively theoretical number of people infected with a contagious illness in a closed population overtime. In the basic model, we assume that the population size is fixed and the incubation period of the infectious agent is instantaneous.

There are three compartments in the fundamental assumption of the compartmental model and they divide the population into distinct groups. The group of individuals that susceptible to the infection of the pathogen (denoted by S); the group of individuals that are already infected and can spread the disease to susceptible group (denoted by I); the group of individuals that are recovered and have the immunity (denoted by R). Because the characteristic of simpleness, the SIR infectious model becomes a common approach. In basic SIR model, we assume that an individual has to be in one of the three groups: S, I, or R. The susceptible individual will become infected individual once they get contact by the disease. Then, the infected individual moves to recovered individual after recovering from the disease.

Then, the differential equations describe this model from [4] are following:

$$\frac{dS}{dt} = \mu N - \frac{\beta SI}{N} - \mu S \quad (1.5a)$$

$$\frac{dI}{dt} = \frac{\beta SI}{N} - \gamma I - \mu I \quad (1.5b)$$

$$\frac{dR}{dt} = \gamma I - \mu R \quad (1.5c)$$

The variables S, I and R are the number of individuals in each class. The total population denoted by N, where $N = S + I + R$. We assume that the population stays constant because per capita population birth and death rate are equal. The term $\frac{\beta SI}{N}$ describes the rate that susceptible individuals become infected individuals. SI means the chance of meeting and β

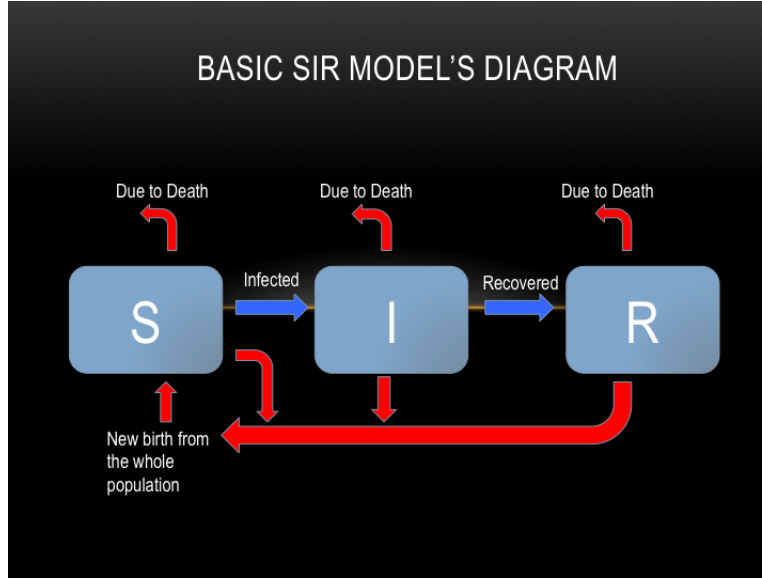


Figure 1.1: Schematic diagram for the SIR model

is the transmission probability. γ is the recovery rate in which γI describes the rate that infected individuals move to recovered individuals.

For SIR model, we investigate the model with incubation period and loss of immunity. Specifically to perform phase plane analysis and find the concept of Basic Reproduction Number (denoted by R_0) for SIR model with time delays. For both of them, we consider the system of ordinary equation with time dependence. In other word, S becomes $S(t)$, I becomes $I(t)$, and R becomes $R(t)$. Applications for SIR model with delays will be provided in this project with numerical results.

1.2.1 Incubation Period

The disease transmission progress plays an important role in the epidemic dynamics. For most of the communicable diseases, there are always different ranges of the incubation period. For example, malaria parasites have a development period within the mosquito before they are infectious to humans. This extrinsic incubation period of the parasite usually ranges from 10 to 28 days. If a female mosquito does not survive longer than the extrinsic incubation period, then this mosquito will not be able to transmit any malaria parasites to other individuals. After a mosquito successfully transfers the parasite to a human body via a bite, there is an intrinsic incubation period, which is the time between the injection of the parasite into the human individual and the development of the first symptoms of malaria. Applying the incubation period into the basic model can change the behaviors of the system. In many epidemic models, SIR models with time delays are widely used in different epidemiological backgrounds. To push the basic models into a more realism level, time delays have been considered into the system. We create another group called exposed group, denoted by E. $E(t)$ is the number of infected individuals that are not infectious at time t . This is also called SEIR model. From this assumption, the delay differential equations can be formed from the

SIR model with the new group E.

$$\frac{dS(t)}{dt} = \mu N(t) - \frac{\beta S(t)I(t)}{N(t)} - \mu S(t) \quad (1.6a)$$

$$\frac{dE(t)}{dt} = \frac{\beta S(t)I(t)}{N(t)} - \frac{\beta S(t-\tau)I(t-\tau)}{N(t)} e^{-\mu\tau} - \mu E(t) \quad (1.6b)$$

$$\frac{dI(t)}{dt} = \frac{\beta S(t-\tau)I(t-\tau)}{N(t)} e^{-\mu\tau} - \gamma I(t) - \mu I(t) \quad (1.6c)$$

$$\frac{dR(t)}{dt} = \gamma I(t) - \mu R(t) \quad (1.6d)$$

where τ is the incubation period that represent the length of time before the infected individuals can become infectious. The term $e^{-\mu\tau}$ describes the fraction of infected people and the people survived at time t . So the term $\frac{\beta S(t-\tau)I(t-\tau)}{N} e^{-\mu\tau}$ conveys the rate of individuals that got infected at τ periods ago and still survive.

Notice that when $\tau = 0$. The exposed class has only $-\mu E(t)$ term; we usually start with $E(0) = 0$. Therefore, we can neglect it. Finally, we get back to the original SIR model.

1.2.2 Loss of Immunity

The SIR model assumes people carry lifelong immunity to a disease upon recovery and this is the case for many diseases. But for another class of diseases, for example seasonal influenza, an individuals immunity may wane over time. Therefore, we have another configuration can be included in SIR model. In this case, the SIRS model is used allow recovered individuals return to a susceptible state. The ordinary differential equations for SIRS model are the following [5]:

$$\frac{dS}{dt} = \mu N - \frac{\beta SI}{N} - \mu S + \alpha R \quad (1.7a)$$

$$\frac{dI}{dt} = \frac{\beta SI}{N} - \gamma I - \mu I \quad (1.7b)$$

$$\frac{dR}{dt} = \gamma I - \mu R - \alpha R \quad (1.7c)$$

All of the terms stays the same in SIR model except αR in susceptible and recovered classes. α represents the rate which recovered individuals return to the susceptible statue due to loss of immunity. Therefore, αR will be the rate that recovered individuals move to susceptible individuals.

However, for many diseases, the recovered individuals will have a time gap before they lose their immunity [6]. So the delay differential equations is

$$\frac{dS(t)}{dt} = \mu N(t) - \frac{\beta S(t)I(t)}{N(t)} - \mu S(t) + \alpha e^{-\mu\omega} R(t-\omega) \quad (1.8a)$$

$$\frac{dI(t)}{dt} = \frac{\beta S(t)I(t)}{N(t)} - \gamma I(t) - \mu I(t) \quad (1.8b)$$

$$\frac{dR(t)}{dt} = \gamma I(t) - \mu R(t) - \alpha e^{-\mu\omega} R(t-\omega) \quad (1.8c)$$

$N(t)$ is the total population at time t . But the population is assumed to be a constant, so $N(t) = S(t) + I(t) + R(t)$ and $N(t_1) = N(t_2)$ for any t_1, t_2 . The $e^{-\mu\omega}$ presents the fraction between recover individual at time $t - \omega$ and survived individual to time t . And ω is the gap time before the recovered individuals loss their immunity. This kind of system is usually called SIRS with delay.

Note that when $\omega = 0$, the last term of susceptible and recovered differential equations will become $\alpha R(t)$ which is exactly the SIRS model. When $\omega = \infty$ or no loss of immunity, the term becomes zero because of the exponential part. Therefore, it goes back to the original SIR model.

1.3 Chemostat model

Competition modeling is one of the most challenging and important aspects of bio-mathematical modeling. In a more nature environment, competition is clearly significant. When we want to model competition in a laboratory device, there is a name of this particular math model, called chemostat model; some may also call it continuous culture. The name Chemostat is originated with Novick and Szilard.

Chemostat model is considerably useful in ecological studies since the mathematics is tractable and the relevant experiments are possible. After this model is getting familiar with more people in math and other science fields, there exist more realistic biological models and many interesting mathematical problems. Chemostat has been widely used to study biological systems and growth of microorganism since the 60's, [7]. It is the simplest technique used to grow microorganisms or cells continually in a particular phase of growth.

We consider the problem of growth of micro-organisms. For a cell to growth, there is a reservoir of limited nutrients. The reservoir is pumped into the cell culture with continuous rate. At the same time, nutrients and cells flow out with the same rate as the pump rate. Therefore the culture contains a constant volume [8].

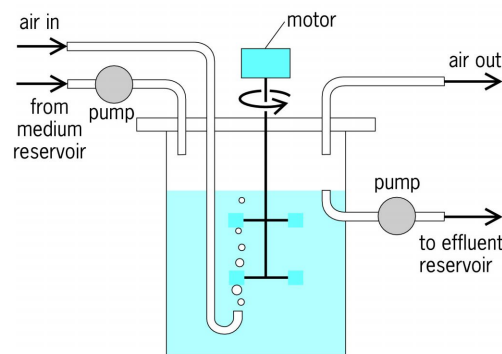


Figure 1.2: A scheme of chemostat [1]

Chemostat model can be constructed as following:

$$\frac{dC(t)}{dt} = \frac{K_1 N(t)}{K_2 + N(t)} C(t) - \frac{F}{V} C(t) \quad (1.9a)$$

$$\frac{dN(t)}{dt} = \frac{F}{V} N_0 - \alpha \frac{K_1 N(t)}{K_2 + N(t)} C(t) - \frac{F}{V} N(t) \quad (1.9b)$$

The term $\frac{K_1 N(t)}{K_2 + N(t)}$ is the growth of cell which satisfies the Michaelis-Menten kinetic, [9]. Therefore, the growth rate of cell is represented by the growth of cell multiplies the density of cell at time t, $\frac{K_1 N(t)}{K_2 + N(t)} C(t)$. Then, the cell get pumped out in the rate $\frac{F}{V} C(t)$.

For nutrient density over time, the rate of pumping nutrients in is $\frac{F}{V} N_0$ and the rate of pumping out is $\frac{F}{V} N(t)$. Then the nutrient is consumed by the cells. The rate of being consumed is defined by the amount nutrient is consumed to produce one unit of cell multiplied by the growth rate of cell: $\alpha \frac{K_1 N(t)}{K_2 + N(t)} C(t)$.

For the simplicity of model, we will non-dimensionalize the chemostat model to the following system:

$$\frac{dX}{dt'} = \frac{\beta Y(t') X(t')}{1 + Y(t')} - X \quad (1.10a)$$

$$\frac{dY}{dt'} = \gamma - Y(t') - \frac{Y(t') X(t')}{1 + Y(t')} \quad (1.10b)$$

where $\beta = \frac{K_1}{\frac{F}{V}}$ and $\gamma = \frac{N_0}{K_2}$. X and Y represent the cell and nutrients, respectively.

$$\begin{aligned} X &= \frac{C}{C^*} \\ Y &= \frac{N}{N^*} \\ t' &= \frac{t}{t^*} \\ C^* &= \frac{K_2 \frac{F}{V}}{\alpha K_1} \\ N^* &= K_2 \\ t^* &= \frac{V}{F} \end{aligned}$$

Now consider that the cell uses ω time to grow after consume the nutrient. Thus, the delay different equations can be introduced as following:

$$\frac{dX}{dt} = e^{-\omega} \frac{\beta Y(t - \omega) X(t - \omega)}{1 + Y(t - \omega)} - X \quad (1.11a)$$

$$\frac{dY}{dt} = \gamma - Y(t) - \frac{Y(t) X(t)}{1 + Y(t)} \quad (1.11b)$$

For this delay differential equations, we have just only two parameter which are β and γ . Therefore, it is obviously easier to work with.

Table 1.1: Introduce the variables and parameters of chemostat model

$C(t)$	Density of cell in the tank at time t
$N(t)$	Density of nutrient in the tank at time t
V	Volume of the tank
N_0	Density of nutrient in the reservoir (constant)
F	Flow rate (pump rate)
α	Amount of nutrient is consumed to produce one unit of cell
K_1	Maximum growth rate
K_2	Nutrient concentration calculated at $1/2$ the maximum growth rate

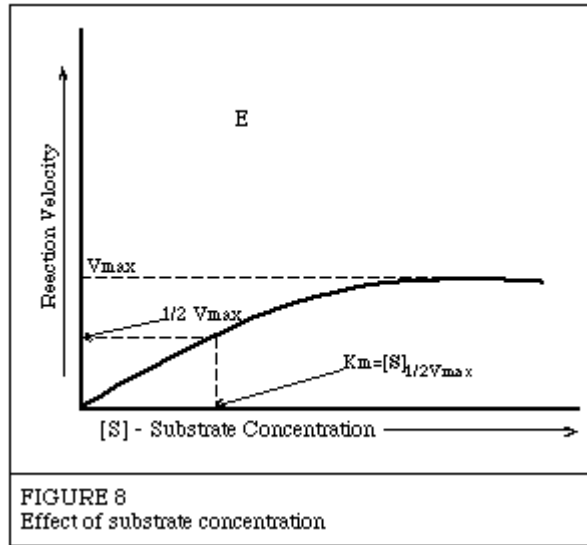


Figure 1.3: Michealis-Menten Kinetic, S in the picture is the same as N in the chemostat model, V_{max} represents K_1 , and K_m represents K_2

Chapter 2

Steady-states and Characteristic Equations

Sometimes, we want to study the qualitative properties of solutions of differential equations, without solving the equations explicitly. Moreover, we often want to know whether a certain property of these solutions remains unchanged if the system is subjected to various changes (often called perturbations). One way to determine those questions is finding the steady-states and the corresponding characteristic equations.

Definition 1. A steady-state for differential equations is a solution where the value does not change over time. For some differential equations

$$\frac{dy}{dt} = F(y)$$

y^* is a steady-state solution of the differential equations if $F(y^*) = 0$, i.e. y^* is a root of $F(y) = 0$.

Definition 2. Let y^* be a steady-state of differential equations. y^* is locally asymptotically stable if there exists a small interval containing y^* such that if $y(0)$ lies in this interval, then $\lim_{t \rightarrow \infty} y(t) = y^*$

Definition 3. Let y^* be a steady-state of differential equations. y^* is unstable if $\lim_{t \rightarrow \infty} y(t) \neq y^*$, no matter how close of $y(0)$ to y^* .

Definition 4. A system of equations has the jacobian matrix. The jacobian matrix of a system is the matrix of the partial derivatives of the right-hand side with respect to state variables. The eigenvalues of the jacobian matrix are the roots of the **characteristic equations**. For ordinary differential equations, the characteristic equations are in form of polynomials. It is less difficult than delay differential equations because theorem of algebra tells us how many roots (eigenvalues) to expect. For the delay differential equation the characteristic equation is transcendental, the number of roots could be countably infinite.

Characteristic equation of the delayed differential equations at its steady-state will have the form

$$P(\lambda, \tau) = P_1(\lambda) + P_2(\lambda)e^{-\lambda\tau} = 0 \quad (2.1)$$

where $P_1(\lambda)$ and $P_2(\lambda)$ are polynomials.

2.1 Logistic growth model with delay

The dimensionless form of the logistic growth model with a constant delay is

$$\frac{dx}{dt} = rx(1 - x(t - \tau)) \quad (2.2)$$

Steady-states and characteristic equations of this model will be useful for analyzing the stability.

2.1.1 Steady-states

Define x^* as the steady-states of the model. Then we can find the steady-states from the solution of the following equation.

$$rx^*(1 - x^*) = 0$$

Therefore, there are two steady-states

$$D_1 : x^* = 0 \quad (2.3)$$

$$D_2 : x^* = 1 \quad (2.4)$$

2.1.2 Characteristic equation

We have to construct A_1 and A_2 from equation 2.2.

$$\begin{aligned} A_1 &= \frac{\partial \frac{dx}{dt}}{\partial x} \\ &= r(1 - x(t - \tau)) \\ &= r(1 - x^*) \\ A_2 &= \frac{\partial \frac{dx}{dt}}{\partial x(t - \tau)} \\ &= -rx \\ &= -rx^* \end{aligned}$$

Then

$$\begin{aligned} J &= A_1 + A_2 e^{-\lambda\tau} \\ &= r(1 - x^*) - rx^* e^{-\lambda\tau} \end{aligned}$$

The characteristic equations is

$$\begin{aligned} P(\lambda, \tau) &= \det(J - \lambda \mathbf{I}) \\ &= J - \lambda = r(1 - x^*) - rx^* e^{-\lambda\tau} - \lambda \end{aligned}$$

since \mathbf{I} and J are scalar

Then the characteristic equations for D_1 and D_2 are

$$P_{D_1}(\lambda, \tau) = r - \lambda \quad (2.5)$$

$$P_{D_2}(\lambda, \tau) = -re^{-\lambda\tau} - \lambda \quad (2.6)$$

These two characteristic can tell how the stability of the solutions is.

2.2 SEIR model with delay

In this paper, we want to study some properties of the susceptible-infected-recovered model with constant incubation period. One thing that we want to study is to determine whether or not varying of delay (incubation period) will affect the stability of solutions. In order to analyze stability of differential equation, we will need the steady-states and characteristic equations from this set of delay differential equations (1.3)

$$\begin{aligned} \frac{dS(t)}{dt} &= \mu N(t) - \frac{\beta S(t)I(t)}{N(t)} - \mu S(t) \\ \frac{dE(t)}{dt} &= \frac{\beta S(t)I(t)}{N(t)} - \frac{\beta S(t-\tau)I(t-\tau)}{N(t)} e^{-\mu\tau} - \mu E(t) \\ \frac{dI(t)}{dt} &= \frac{\beta S(t-\tau)I(t-\tau)}{N(t)} e^{-\mu\tau} - \gamma I(t) - \mu I(t) \\ \frac{dR(t)}{dt} &= \gamma I(t) - \mu R(t) \end{aligned}$$

2.2.1 Steady-states

Before we can find the steady-states of these differential equations, we need to simplify the equations as much as we can. First of all, since we have a constant population $N(t) = N = S(t) + E(t) + I(t) + R(t)$, we have $R(t) = N - S(t) + E(t) + I(t)$. Therefore, we can omit $\frac{dR(t)}{dt}$ equation. Secondly, there is no $E(t)$ term in other equations except $\frac{dE(t)}{dt}$, derivative of itself. So we can find $E(t)$ once we know $S(t)$ and $I(t)$. That means the only equations that we are going to consider are $\frac{dS(t)}{dt}$ and $\frac{dI(t)}{dt}$. Now let

$$\begin{aligned} \lim_{t \rightarrow \infty} S(t) &= \lim_{t \rightarrow \infty} S(t - \tau) = S^* \\ \lim_{t \rightarrow \infty} I(t) &= \lim_{t \rightarrow \infty} I(t - \tau) = I^* \end{aligned}$$

Then, the steady-states can be calculated by setting $\frac{dS(t)}{dt}$ and $\frac{dI(t)}{dt}$ to be zero.

$$\mu N - \frac{\beta S^* I^*}{N} - \mu S^* = 0 \quad (2.8a)$$

$$\frac{\beta S^* I^*}{N} e^{-\mu\tau} - \gamma I^* - \mu I^* = 0 \quad (2.8b)$$

From equation 2.8b, we have

$$\begin{aligned} \frac{\beta S^* I^*}{N} e^{-\mu\tau} - \gamma I^* - \mu I^* &= 0 \\ \Leftrightarrow I^* \left(\frac{\beta S^*}{N} e^{-\mu\tau} - \gamma - \mu \right) &= 0 \end{aligned} \quad (2.9)$$

There are two cases: one is $I^* = 0$, and another one is $S^* = \frac{N}{R_0^{delay}}$, where $R_0^{delay} = \frac{\beta}{\mu + \gamma} e^{-\mu\tau}$.

Substitute $I^* = 0$ into equation 2.8a.

$$\begin{aligned} \mu N - \frac{\beta S^*(0)}{N} - \mu S^* &= 0 \\ \mu N - \mu S^* &= 0 \\ S^* &= N \end{aligned}$$

The first steady-state (S^*, I^*) is

$$E_1 = (N, 0) \quad (2.10)$$

Substitute $S^* = \frac{N}{R_0^{delay}}$ into equation 2.8a.

$$\begin{aligned} \mu N - \frac{\beta \frac{N}{R_0^{delay}} I^*}{N} - \mu \frac{N}{R_0^{delay}} &= 0 \\ \frac{\beta I^*}{R_0^{delay}} &= \mu N - \mu \frac{N}{R_0^{delay}} \\ I^* &= \frac{\mu N}{\beta} (R_0^{delay} - 1) \end{aligned}$$

The second steady-state (S^*, I^*) is

$$E_2 = \left(\frac{N}{R_0^{delay}}, \frac{\mu N}{\beta} (R_0^{delay} - 1) \right) \quad (2.11)$$

Notice that, if $R_0^{delay} < 1$, then $I^* < 0$ and $S^* > N$ for steady-state E_2 which is impossible. It implies that E_2 exists if $R_0^{delay} > 1$. (If $R_0^{delay} = 1$, $E_2 = E_1$.) We call R_0^{delay} as the basic reproduction number.

2.2.2 Characteristic equation

After we obtain two steady-states, we want to study about their stability. Therefore, finding characteristic equation for each steady-state will be a method for the goal.

To construct a characteristic equation, two matrices A_1 and A_2 have to be computed.

$$\begin{aligned}
A_1 &= \begin{bmatrix} \frac{\partial \frac{dS(t)}{dt}}{\partial S(t)} & \frac{\partial \frac{dS(t)}{dt}}{\partial I(t)} \\ \frac{\partial \frac{dI(t)}{dt}}{\partial S(t)} & \frac{\partial \frac{dI(t)}{dt}}{\partial I(t)} \end{bmatrix} \\
&= \begin{bmatrix} -\frac{\beta I(t)}{N} - \mu & -\frac{\beta S(t)}{N} \\ 0 & -\mu - \gamma \end{bmatrix} \\
&= \begin{bmatrix} -\frac{\beta I^*}{N} - \mu & -\frac{\beta S^*}{N} \\ 0 & -\mu - \gamma \end{bmatrix} \\
A_2 &= \begin{bmatrix} \frac{\partial \frac{dS(t)}{dt}}{\partial S(t-\tau)} & \frac{\partial \frac{dS(t)}{dt}}{\partial I(t-\tau)} \\ \frac{\partial \frac{dI(t)}{dt}}{\partial S(t-\tau)} & \frac{\partial \frac{dI(t)}{dt}}{\partial I(t-\tau)} \end{bmatrix} \\
&= \begin{bmatrix} 0 & 0 \\ \frac{\beta I(t-\tau)e^{-\mu\tau}}{N} & \frac{\beta S(t-\tau)e^{-\mu\tau}}{N} \end{bmatrix} \\
&= \begin{bmatrix} 0 & 0 \\ \frac{\beta I^*e^{-\mu\tau}}{N} & \frac{\beta S^*e^{-\mu\tau}}{N} \end{bmatrix}
\end{aligned}$$

then the jacobian matrix of the differential equations is

$$\begin{aligned}
J &= A_1 + A_2e^{-\lambda\tau} \\
&= \begin{bmatrix} -\frac{\beta I^*}{N} - \mu & -\frac{\beta S^*}{N} \\ \frac{\beta I^*e^{-\mu\tau}e^{-\lambda\tau}}{N} & -\mu - \gamma + \frac{\beta S^*e^{-\mu\tau}e^{-\lambda\tau}}{N} \end{bmatrix}
\end{aligned}$$

For each steady-state, we have

$$J_{E_1} = \begin{bmatrix} -\mu & -\beta \\ 0 & -\mu - \gamma + \beta e^{-\mu\tau}e^{-\lambda_{E_1}\tau} \end{bmatrix} \quad (2.12)$$

$$J_{E_2} = \begin{bmatrix} -\mu R_0^{delay} & -\frac{\beta}{R_0^{delay}} \\ \mu R_0^{delay}e^{-\mu\tau}e^{-\lambda\tau} & -\mu - \gamma + \frac{\beta e^{-\mu\tau}e^{-\lambda\tau}}{R_0^{delay}} \end{bmatrix} \quad (2.13)$$

Then, the characteristic equations can be calculated from this

$$P(\lambda, \tau) = \det(J - \lambda \mathbf{I}) = 0$$

where \mathbf{I} is the identity matrix with the same size as J , and λ is the eigenvalues to J .

Since we have two steady-states, we have two characteristic equations. The first characteristic equation with respect to E_1 is:

$$\begin{aligned} P_{E_1}(\lambda, \tau) &= \det(J_{E_1} - \lambda \mathbf{I}) \\ &= \lambda^2 + (2\mu + \gamma - e^{-\lambda\tau} \beta e^{-\mu\tau}) \lambda - (-\mu - \gamma + e^{-\lambda\tau} \beta e^{-\mu\tau}) \mu \end{aligned}$$

Therefore, we can separate it into $P_1(\lambda)$ and $P_2(\lambda)$ as following:

$$\begin{aligned} P_{1,E_1}(\lambda) &= \lambda^2 + (2\mu + \gamma) \lambda - (-\mu - \gamma) \mu \\ P_{2,E_1}(\lambda) &= -\beta e^{-\mu\tau} \lambda - \beta e^{-\mu\tau} \mu \end{aligned}$$

Thus, the second characteristic equation with respect to E_2 is:

$$\begin{aligned} P_{E_2}(\lambda, \tau) &= \det(J_{E_2} - \lambda \mathbf{I}) \\ &= \lambda^2 + \frac{((\mu + \gamma)^2 - (\mu + \gamma)^2 e^{-\lambda\tau} + \mu \beta e^{-\mu\tau}) \lambda}{\mu + \gamma} + ((-\mu - \gamma) e^{-\lambda\tau} + \beta e^{-\mu\tau}) \mu \end{aligned} \quad (2.14)$$

Therefore, we can separate it into $P_1(\lambda)$ and $P_2(\lambda)$ as following:

$$\begin{aligned} P_{1,E_2}(\lambda) &= \lambda^2 + (\mu + \gamma + \frac{\mu \beta e^{-\mu\tau}}{\mu + \gamma}) \lambda + \mu \beta e^{-\mu\tau} \\ &= \lambda^2 + (\mu + \gamma + \mu R_0^{delay}) \lambda + \mu \beta e^{-\mu\tau} \end{aligned} \quad (2.15)$$

$$P_{2,E_2}(\lambda) = (-\mu - \gamma) \lambda + (-\mu - \gamma) \mu \quad (2.16)$$

We can conclude that characteristic equations both have quadratic polynomial for $P_1(\lambda)$ and linear polynomial for $P_2(\lambda)$.

2.3 SIRS model with delay

As the same goal as SEIR model, finding steady-states and characteristic equations from the system of differential equations for loss of immunity from (1.8) is necessary.

$$\begin{aligned} \frac{dS(t)}{dt} &= \mu N(t) - \frac{\beta S(t) I(t)}{N(t)} - \mu S(t) + \alpha e^{-\mu\omega} R(t - \omega) \\ \frac{dI(t)}{dt} &= \frac{\beta S(t) I(t)}{N(t)} - \gamma I(t) - \mu I(t) \\ \frac{dR(t)}{dt} &= \gamma I(t) - \mu R(t) - \alpha e^{-\mu\omega} R(t - \omega) \end{aligned}$$

2.3.1 Steady-states

We know that $\alpha R(t - \omega)$ represents the temporary immunity. We want to find out in the stability analysis which is the critical value of the ω that cause the system of equations to have or not a periodic solution.

We know that we have a constant population $N(t) = N = S(t) + E(t) + I(t) + R(t)$, we have $R(t) = N - S(t) + E(t) + I(t)$. Therefore, we begins with changing the first differential equation into this form

$$\frac{dS(t)}{dt} = \mu N - \frac{\beta S(t)I(t)}{N} - \mu S(t) + \alpha e^{-\mu\omega}(N - S(t - \omega) - I(t - \omega)) \quad (2.18)$$

Then the steady-states of these delay differential equation can be simplified by considering only $\frac{dS(t)}{dt}$ and $\frac{dI(t)}{dt}$. (We can find $R(t)$ after we know $S(t)$ and $I(t)$.)

Define the steady-states as the following:

$$\begin{aligned} \lim_{t \rightarrow \infty} S(t) &= \lim_{t \rightarrow \infty} S(t - \tau) = S^* \\ \lim_{t \rightarrow \infty} I(t) &= \lim_{t \rightarrow \infty} I(t - \tau) = I^* \end{aligned}$$

Then, we find the steady-states by taking $\frac{dS(t)}{dt}$ and $\frac{dI(t)}{dt}$ at the steady-state (S^*, I^*) to be zero.

$$\mu N - \frac{\beta S^* I^*}{N} - \mu S^* + \alpha e^{-\mu\omega}(N - S^* - I^*) = 0 \quad (2.19)$$

$$\frac{\beta S^* I^*}{N} - \gamma I^* - \mu I^* = 0 \quad (2.20)$$

From equation (2.20), we can conclude that the equation will become zero either $I^* = 0$ or $S^* = N \frac{(\mu + \gamma)}{\beta}$.

When $I^* = 0$, equation (2.19) becomes

$$\begin{aligned} \mu N - \mu S^* + \alpha e^{-\mu\omega}(N - S^*) &= 0 \\ (\mu + \alpha e^{-\mu\omega})(N - S^*) &= 0 \end{aligned}$$

Thus, our first steady-state (S^*, I^*) for SIRS model is

$$E_3 = (N, 0) \quad (2.21)$$

Then consider $S^* = N \frac{(\mu + \gamma)}{\beta}$. The basic reproduction number in SIRS model is actually the same as SIR model, the basic disease model, which is $\frac{\beta}{(\mu + \gamma)}$. Therefore, $S^* = \frac{N}{R_0}$.

Substitute this S^* into equation (2.19).

$$\begin{aligned}
\mu N - \mu \frac{N}{R_0} + \alpha e^{-\mu\omega} \left(N - \frac{N}{R_0}\right) - \frac{\beta \frac{N}{R_0} I^*}{N} - \alpha e^{-\mu\omega} I^* &= 0 \\
(\mu + \alpha e^{-\mu\omega}) \left(N - \frac{N}{R_0}\right) &= I^* \left(\frac{\beta}{R_0} + \alpha e^{-\mu\omega}\right) \\
\frac{(\mu + \alpha e^{-\mu\omega}) \left(N - \frac{N}{R_0}\right)}{\left(\frac{\beta}{R_0} + \alpha e^{-\mu\omega}\right)} &= I^* \\
\frac{N(\mu + \alpha e^{-\mu\omega})(R_0 - 1)}{(\beta + R_0 \alpha e^{-\mu\omega})} &= I^*
\end{aligned}$$

Thus, our second steady-state for this SIRS model is

$$E_4 = \left(\frac{N}{R_0}, \frac{(R_0 - 1)(\mu + \alpha e^{-\mu\omega})}{(\beta + R_0 \alpha e^{-\mu\omega})} \right) \quad (2.22)$$

2.3.2 Characteristic equation

Again we construct two matrices.

$$\begin{aligned}
A_1 &= \begin{bmatrix} \frac{\partial \frac{dS(t)}{dt}}{\partial S(t)} & \frac{\partial \frac{dS(t)}{dt}}{\partial I(t)} \\ \frac{\partial \frac{dI(t)}{dt}}{\partial S(t)} & \frac{\partial \frac{dI(t)}{dt}}{\partial I(t)} \end{bmatrix} \\
&= \begin{bmatrix} -\frac{\beta I(t)}{N} - \mu & -\frac{\beta S(t)}{N} \\ \frac{\beta I(t)}{N} & -\mu - \gamma + \frac{\beta S(t)}{N} \end{bmatrix} \\
&= \begin{bmatrix} -\frac{\beta I^*}{N} - \mu & -\frac{\beta S^*}{N} \\ \frac{\beta I^*}{N} & -\mu - \gamma + \frac{\beta S^*}{N} \end{bmatrix} \\
A_2 &= \begin{bmatrix} \frac{\partial \frac{dS(t)}{dt}}{\partial S(t-\tau)} & \frac{\partial \frac{dS(t)}{dt}}{\partial I(t-\tau)} \\ \frac{\partial \frac{dI(t)}{dt}}{\partial S(t-\tau)} & \frac{\partial \frac{dI(t)}{dt}}{\partial I(t-\tau)} \end{bmatrix} \\
&= \begin{bmatrix} -\alpha e^{-\mu\omega} & -\alpha e^{-\mu\omega} \\ 0 & 0 \end{bmatrix}
\end{aligned}$$

The jacobian matrix of the differential equations is

$$\begin{aligned}
J &= A_1 + A_2 e^{-\lambda\omega} \\
&= \begin{bmatrix} -\frac{\beta I^*}{N} - \mu - \alpha e^{-\mu\omega} e^{-\lambda\omega} & -\frac{\beta S^*}{N} - \alpha e^{-\mu\omega} e^{-\lambda\omega} \\ \frac{\beta I^*}{N} & -\mu - \gamma + \frac{\beta S^*}{N} \end{bmatrix}
\end{aligned} \quad (2.23)$$

For each steady-state, we have

$$J_{E_3} = \begin{bmatrix} -\mu - \alpha e^{-\mu\omega} e^{-\lambda\omega} & -\beta - \alpha e^{-\mu\omega} e^{-\lambda\omega} \\ 0 & -\mu - \gamma + \beta \end{bmatrix} \quad (2.24)$$

$$J_{E_4} = \begin{bmatrix} -\beta \frac{(R_0 - 1)(\mu + \alpha e^{-\mu\omega})}{(\beta + R_0 \alpha e^{-\mu\omega})} - \mu - \alpha e^{-\mu\omega} e^{-\lambda\omega} & -\frac{\beta}{R_0} - \alpha e^{-\mu\omega} e^{-\lambda\omega} \\ \beta \frac{(R_0 - 1)(\mu + \alpha e^{-\mu\omega})}{(\beta + R_0 \alpha e^{-\mu\omega})} & 0 \end{bmatrix} \quad (2.25)$$

The characteristic equation is

$$P(\lambda, \omega) = \det(J - \lambda \mathbf{I}) = 0$$

There are two characteristic equations. The first characteristic equation with respect to E_3 is:

$$\begin{aligned} P_{E_3}(\lambda, \omega) &= \det(J_{E_3} - \lambda \mathbf{I}) \\ &= (-\mu - \alpha e^{-\mu\omega} e^{-\lambda\omega} - \lambda)(\beta - \mu - \gamma - \lambda) \end{aligned} \quad (2.26)$$

The second characteristic equation with respect to E_4 is:

$$\begin{aligned} P_{E_4}(\lambda, \omega) &= \det(J_{E_4} - \lambda \mathbf{I}) \\ &= (M - \mu - \alpha e^{-\mu\omega} e^{-\lambda\omega} - \lambda)(-\lambda) - M(-\frac{\beta}{R_0} - \alpha e^{-\mu\omega} e^{-\lambda\omega}) \\ &= \lambda^2 - (M - \mu)\lambda + \frac{\beta}{R_0} M + \alpha e^{-\mu\omega} e^{-\lambda\omega} \lambda + M \alpha e^{-\mu\omega} e^{-\lambda\omega} \end{aligned} \quad (2.27)$$

where

$$M = \beta \frac{(R_0 - 1)(\mu + \alpha e^{-\mu\omega})}{(\beta + R_0 \alpha e^{-\mu\omega})} \quad (2.28)$$

Therefore, we can separate it into $P_1(\lambda)$ and $P_2(\lambda)$ as following:

$$P_{1,E_4}(\lambda) = \lambda^2 - (M - \mu)\lambda + \frac{\beta}{R_0} M \quad (2.29)$$

$$P_{2,E_4}(\lambda) = \alpha e^{-\mu\omega} \lambda + M \alpha e^{-\mu\omega} \quad (2.30)$$

where

$$P_{E_4}(\lambda) = P_{1,E_4}(\lambda) + P_{2,E_4}(\lambda) e^{-\lambda\omega}$$

Consequently, we have quadratic polynomial for $P_1(\lambda)$ and linear polynomial for $P_2(\lambda)$ for each characteristic polynomials as same as in SEIR model.

2.4 Chemostat model with delay

The steady-states and characteristic equations of Chemostat model will provide our information about how the delay in growing part affects the stability of its solutions.

2.4.1 Steady-states

Consider the dimensionless form of the chemostat model 1.11.

$$\begin{aligned}\frac{dX}{dt} &= e^{-\omega} \frac{\beta Y(t-\omega)X(t-\omega)}{1+Y(t-\omega)} - X \\ \frac{dY}{dt} &= \gamma - Y(t) - \frac{Y(t)X(t)}{1+Y(t)}\end{aligned}$$

Assume that

$$\begin{aligned}\lim_{t \rightarrow \infty} X(t) &= \lim_{t \rightarrow \infty} X(t-\omega) = X^* \\ \lim_{t \rightarrow \infty} Y(t) &= \lim_{t \rightarrow \infty} Y(t-\omega) = Y^*\end{aligned}$$

Steady-states are X^* and Y^* that satisfy the equations $\frac{dX}{dt} = 0$ and $\frac{dY}{dt} = 0$. Consider equation $\frac{dX}{dt} = 0$.

$$e^{-\omega} \frac{\beta Y^* X^*}{1+Y^*} - X^* = (e^{-\omega} \frac{\beta Y^*}{1+Y^*} - 1) X^* = 0 \quad (2.32)$$

Therefore, the first steady-state has $X^* = 0$. Then the corresponding Y^* of this X^* can be obtained by substituting X^* into equation $\frac{dY}{dt} = 0$. As the result, $Y^* = \gamma$. To conclude, the first steady-state is

$$F_1 = (0, \gamma) \quad (2.33)$$

The first part of the second steady-state obtained from equation 2.32 is $Y^* = \frac{1}{\beta e^{-\omega} - 1}$. Then, by substituting Y^* into $\frac{dY}{dt} = 0$, X^* in this situation is $\beta e^{-\omega}(\gamma - \frac{1}{\beta e^{-\omega} - 1})$. We multiply this formula by $\frac{\beta e^{-\omega} - 1}{\beta e^{-\omega} - 1}$ and have $X^* = \frac{\beta e^{-\omega}}{\beta e^{-\omega} - 1}((\beta e^{-\omega} - 1)\gamma - 1)$. Notice that X^* is positive if and only if $(\beta e^{-\omega} - 1)\gamma > 1$. Let $R_0 = (\beta e^{-\omega} - 1)\gamma$. Then the second steady-state is

$$F_2 = (\frac{\beta e^{-\omega}}{\beta e^{-\omega} - 1}(R_0 - 1), \frac{1}{\beta e^{-\omega} - 1})$$

We can simplify this a little more. Let $H = 1 + \frac{1}{\beta e^{-\omega} - 1}$. Then F_2 becomes

$$F_2 = (H(R_0 - 1), H - 1) \quad (2.34)$$

2.4.2 Characteristic equation

First of all, construct two matrices A_1 and A_2 .

$$\begin{aligned}
A_1 &= \begin{bmatrix} \frac{\partial \frac{dX(t)}{dt}}{\partial X(t)} & \frac{\partial \frac{dX(t)}{dt}}{\partial Y(t)} \\ \frac{\partial \frac{dY(t)}{dt}}{\partial X(t)} & \frac{\partial \frac{dY(t)}{dt}}{\partial Y(t)} \end{bmatrix} \\
&= \begin{bmatrix} -1 & 0 \\ \frac{Y(t)}{1+Y(t)} & -1 - \frac{X(t)}{(1+Y(t))^2} \end{bmatrix} \\
&= \begin{bmatrix} -1 & 0 \\ \frac{Y^*}{1+Y^*} & -1 - \frac{X^*}{(1+Y^*)^2} \end{bmatrix} \\
A_2 &= \begin{bmatrix} \frac{\partial \frac{dX(t)}{dt}}{\partial X(t-\omega)} & \frac{\partial \frac{dX(t)}{dt}}{\partial Y(t-\omega)} \\ \frac{\partial \frac{dY(t)}{dt}}{\partial X(t-\omega)} & \frac{\partial \frac{dY(t)}{dt}}{\partial Y(t-\omega)} \end{bmatrix} \\
&= \begin{bmatrix} \frac{\beta Y(t-\omega)}{1+Y(t-\omega)} e^{-\omega} & \frac{\beta X(t-\omega)}{(1+Y(t-\omega))^2} e^{-\omega} \\ 0 & 0 \end{bmatrix} \\
&= \begin{bmatrix} \frac{\beta Y^*}{1+Y^*} e^{-\omega} & \frac{\beta X^*}{(1+Y^*)^2} e^{-\omega} \\ 0 & 0 \end{bmatrix}
\end{aligned}$$

The jacobian matrix of the differential equations is obtained by following:

$$\begin{aligned}
J &= A_1 + A_2 e^{-\lambda\omega} \\
&= \begin{bmatrix} -1 + \frac{\beta Y^*}{1+Y^*} e^{-\omega} e^{-\lambda\omega} & \frac{\beta X^*}{(1+Y^*)^2} e^{-\omega} e^{-\lambda\omega} \\ -\frac{Y^*}{1+Y^*} & -1 - \frac{X^*}{(1+Y^*)^2} \end{bmatrix}
\end{aligned}$$

Considering the jacobian matrix for each steady-state, we have

$$J_{F_1} = \begin{bmatrix} -1 + \frac{\beta\gamma}{1+\gamma} e^{-\omega} e^{-\lambda\omega} & 0 \\ -\frac{\gamma}{1+\gamma} & -1 \end{bmatrix} \quad (2.35)$$

$$J_{F_2} = \begin{bmatrix} -1 + \frac{\beta(H-1)}{H} e^{-\omega} e^{-\lambda\omega} & \frac{\beta H(R_0-1)}{H^2} e^{-\omega} e^{-\lambda\omega} \\ -\frac{H-1}{H} & -1 - \frac{H(R_0-1)}{H^2} \end{bmatrix} \quad (2.36)$$

Then, the characteristic equations can be calculated from

$$P(\lambda, \tau) = \det(J - \lambda \mathbf{I}) = 0$$

where \mathbf{I} is the 2x2 identity matrix, and λ is the eigenvalues.

The two characteristic equations: characteristic equation with respect to F_1 is

$$\begin{aligned} P_{F_1}(\lambda, \tau) &= \det(J_{F_1} - \lambda \mathbf{I}) \\ &= \lambda^2 + 2\lambda + 1 + \left(-\frac{\gamma\beta e^{-\omega}}{1+\gamma}\lambda - \frac{\gamma\beta e^{-\omega}}{1+\gamma} \right) e^{-\lambda\omega} \end{aligned} \quad (2.37)$$

characteristic equation with respect to F_2 is

$$\begin{aligned} P_{F_2}(\lambda, \tau) &= \det(J_{F_2} - \lambda \mathbf{I}) \\ &= \lambda^2 + \left(2 + \frac{R_0 - 1}{H} \right) \lambda + 1 + \frac{R_0 - 1}{H} + \left(-\beta e^{-\omega} \left(1 - \frac{1}{H} \right) (\lambda + 1) \right) e^{-\lambda\omega} \end{aligned} \quad (2.38)$$

Notice that both characteristic equations have the quadratic polynomial parts for the term without $e^{-\lambda\omega}$, and the parts with $e^{-\lambda\omega}$ are linear polynomial. After obtain the characteristic equations, we will use them for stability properties of F_1 and F_2 .

Chapter 3

Stability Analysis

Delay differential equations are often of interest to determine whether or not the delay value affects the stability of a steady-state. In this paper, the delay has been treated as a bifurcation parameter.

Our objective is to determine whether or not a stable steady-state can become unstable by changing the delay value. Therefore, we will look at the eigenvalues from roots of characteristic equations. If all the roots have negative real part, the steady-state is stable. When we vary the delay, if one of the root changes from having negative real part to having positive real part because of the delay, it implies that the steady-state will become unstable. This is also equivalent to having the root crossing the imaginary-axis (imagine the root as a graph with real part on x-axis and imaginary part on y-axis). Therefore, if the root really turns to be positive, there must be a root that is purely imaginary part. (i.e. the intersection between the graph of the root and the imaginary-axis exist.) It is important to prove that the root continues into positive side of the graph when increasing the delay value. The proof can be found in Chapter 2 section 1.2. of [10].

We know that a characteristic equation of the delay differential equations can be written in the form (2.1), and we are looking for a purely imaginary root, $i\sigma, \sigma \in \mathbb{R}$. Therefore, we have this form:

$$P_1(i\sigma) + P_2(i\sigma)e^{-i\sigma\tau} = 0 \quad (3.1)$$

This is one of the tool that we will use to check the stability. It comes from Forde's Ph.D. thesis. From (3.1), we can split each polynomial into the real and imaginary parts. Moreover, the exponential part can be expanded by Euler's formula.

$$R_1(\sigma) + iQ_1(\sigma) + (R_2(\sigma) + iQ_2(\sigma))(\cos(\sigma\tau) - i\sin(\sigma\tau)) = 0 \quad (3.2)$$

where $R_1(\sigma)$ and $Q_1(\sigma)$ are the real part and imaginary part (with i) respectively from $P_1(i\sigma)$. The same goes for $R_2(\sigma)$, $Q_2(\sigma)$ and $P_2(i\sigma)$.

This equation equals to zero if and only if the real part and imaginary part both have to be zero. Therefore, we obtain two equations:

$$-R_1(\sigma) = R_2(\sigma)\cos(\sigma\tau) + Q_2(\sigma)\sin(\sigma\tau) \quad (3.3)$$

$$Q_1(\sigma) = R_2(\sigma)\sin(\sigma\tau) - Q_2(\sigma)\cos(\sigma\tau) \quad (3.4)$$

After that we square equations 3.3 and 3.4. We will have as the following:

$$R_1^2(\sigma) = R_2^2(\sigma)\cos^2(\sigma\tau) + Q_2^2(\sigma)\sin^2(\sigma\tau) + 2R_2(\sigma)Q_2(\sigma)\sin(\sigma\tau)\cos(\sigma\tau) \quad (3.5)$$

$$Q_1^2(\sigma) = R_2^2(\sigma)\sin^2(\sigma\tau) + Q_2^2(\sigma)\cos^2(\sigma\tau) - 2R_2(\sigma)Q_2(\sigma)\sin(\sigma\tau)\cos(\sigma\tau) \quad (3.6)$$

Add equations 3.5 and 3.6 together. The last part of each equation will cancel each other. The result is

$$\begin{aligned} R_1^2(\sigma) + Q_1^2(\sigma) &= R_2^2(\sigma)(\cos^2(\sigma\tau) + \sin^2(\sigma\tau)) + Q_2^2(\sigma)(\cos^2(\sigma\tau) + \sin^2(\sigma\tau)) \\ &= R_2^2(\sigma) + Q_2^2(\sigma) \end{aligned} \quad (3.7)$$

Therefore, the purely imaginary number is a root of the characteristic equation if this formula holds.

Let a variable $z = \sigma^2$. Then define equation 3.7 as a function S.

$$S(z) = R_1^2(\sigma) + Q_1^2(\sigma) - (R_2^2(\sigma) + Q_2^2(\sigma)) = 0 \quad (3.8)$$

We know $\sigma \in \mathbb{R}$. If all of the real roots z of $S(z)$ are negative, then such a σ cannot exist. Therefore, the roots λ of the characteristic equations will not change from having negative real parts to having positive real part. That means the model does not have a Hopf bifurcation regardless of τ value. However, if there exists a real root z^* that is positive, then $\sigma^* = \pm\sqrt{z^*}$. Thus, we can find a τ^* corresponding to that σ^* . Then the periodic solutions start to happen at that τ^* , called critical delay.

3.1 Logistic growth model with delay

The characteristic equations give us the eigenvalues. It is obviously that $\lambda = r > 0$ for steady-state D_1 . Therefore, The steady-state D_1 is unstable. So we will not consider steady-state D_1 .

Our interesting case is steady-state D_2 . We want to find the value of τ that cause its characteristic equation 2.6 to change from having positive real part to having negative real part for eigenvalue. It implies that the root of the characteristic equation will cross from left-half to right-half of complex plane. Therefore, if this really happens, then the purely imaginary eigenvalue must exist.

From this fact, we assume that $\lambda = \sigma i$. Thus, from the Euler's formula, we obtain

$$\begin{aligned} i\sigma &= -re^{-i\tau\sigma} \\ &= -r(\cos(\tau\sigma) - i\sin(\tau\sigma)) \end{aligned}$$

Then, this equation can be true if and only if the two equations satisfy.

$$0 = -r\cos(\tau\sigma) \quad (3.9)$$

$$\sigma = r\sin(\tau\sigma) \quad (3.10)$$

From equation 3.9, we have

$$\tau\sigma = \frac{\pi}{2}(2k - 1) \quad (3.11)$$

where $k \in \mathbb{Z}^+$

The critical delay τ^* is $\frac{\pi}{2\sigma}$. Then we can substitute this critical delay back to equation 3.10. As the result, we have $\sigma = r$.

For example, take $r = 2$, then the critical delay is $\tau^* = \frac{\pi}{4}$. There is a Hopf bifurcation at $\tau = \frac{\pi}{4}$. If τ is greater than τ^* , then the periodic solution occurs. Otherwise, the solution is still stable at steady-state D_2 . These are shown in figures 3.1 and 3.2.

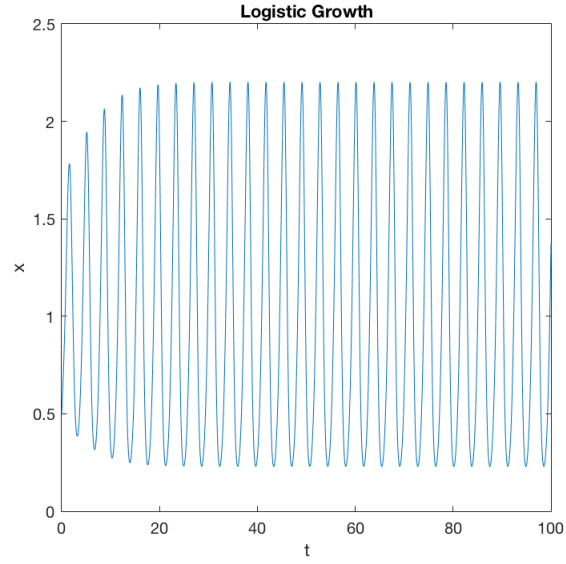


Figure 3.1: $\tau = \frac{\pi}{4} + 0.1$

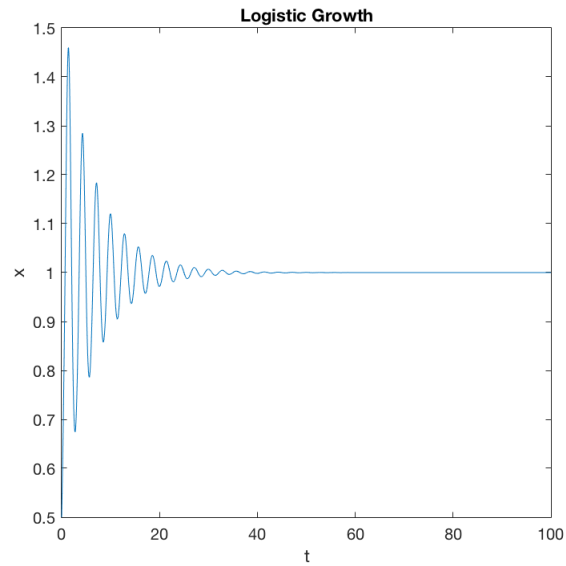


Figure 3.2: $\tau = \frac{\pi}{4} - 0.1$

3.2 SEIR model with delay

We want to determine whether or not each steady-state of SEIR model will change from stable to unstable by increasing the delay value (τ).

3.2.1 Steady-state E_1

First we look at the steady-state E_1 . If there is no delay (i.e. $\tau = 0$), we know that E_1 will be stable when R_0^{delay} less than 1. Therefore, we will test whether or not this steady-state will change from being stable to begin unstable. Consider the jacobian matrix J_{E_1} from (2.12). The characteristic equation can also be in this form.

$$P_{E_1}(\lambda, \tau) = (-\mu - \lambda)(-\mu - \gamma + \beta e^{-\mu\tau} e^{-\lambda\tau} - \lambda) = 0 \quad (3.12)$$

We can conclude that one of the eigenvalues is $-\mu$. If the other eigenvalues also have negative real part, then we can confirm that there is no Hopf bifurcation for E_1 .

$$\begin{aligned} -\mu - \gamma + \beta e^{-\mu\tau} e^{-\lambda\tau} - \lambda &= 0 \\ \Leftrightarrow \lambda &= -\mu - \gamma + \beta e^{-\mu\tau} e^{-\lambda\tau} \\ &= -(\mu + \gamma) \left(1 - \frac{\beta e^{-\mu\tau}}{\mu + \gamma} e^{-\lambda\tau}\right) \\ &= -(\mu + \gamma) (1 - R_0^{delay} e^{-\lambda\tau}) \end{aligned} \quad (3.13)$$

$$\Leftrightarrow \frac{\lambda}{\mu + \gamma} = R_0^{delay} e^{-\lambda\tau} - 1 \quad (3.14)$$

Let

$$x = R_0^{delay} e^{-\lambda\tau}$$

Suppose that this λ has positive real part. $\lambda = a + ib$ where a is zero or positive real number and b is a real number. Then the magnitude of x is following:

$$|x| = R_0^{delay} e^{-a\tau} |e^{-bi\tau}|$$

Since $e^{-bi\tau} = \cos(b\tau) - i\sin(b\tau)$, $|e^{-bi\tau}| = 1$. Then

$$|x| = R_0^{delay} e^{-a\tau} \leq R_0^{delay} < 1$$

Therefore, the right hand side of equation (3.14), $x - 1$, is a complex number in the left-half of complex plane. Then consider the left hand side of the equation.

$$\frac{\lambda}{\mu + \gamma} = \frac{a}{\mu + \gamma} + \frac{b}{\mu + \gamma}i$$

We suppose that $\frac{a}{\mu + \gamma} > 0$, then $\frac{\lambda}{\mu + \gamma}$ will be a complex number on the right-half of complex plane. This contradicts with the right hand side of the equation.

We conclude, by contradiction, that a cannot be a positive real number. The eigenvalues of this characteristic equation will never cross from left-half to right-half of complex plane. Then, there is not a Hopf bifurcation; E_1 will be stable regardless of the delay value, τ .

3.2.2 Steady-state E_2

Again we know that when $\tau = 0$ and R_0^{delay} greater than 1, E_2 will be stable. The jacobian matrix J_{E_2} (2.13) can provide the characteristic equation (2.14), and then equation 2.15 and 2.16. In this case, we will use the tool (3.1) to check the stability. The equation (2.14) becomes

$$\begin{aligned} P_{1,E_2}(i\sigma) &= -\sigma^2 + i(\mu + \gamma + \mu R_0^{delay})\sigma + \mu\beta e^{-\mu\tau} \\ P_{2,E_2}(i\sigma) &= i(-\mu - \gamma)\sigma + (-\mu - \gamma)\mu \end{aligned}$$

Then, we can break them as in (3.2). Therefore, we have

$$\begin{aligned} R_1(\sigma) &= -\sigma^2 + \mu\beta e^{-\mu\tau} \\ Q_1(\sigma) &= (\mu + \gamma + \mu R_0^{delay})\sigma \\ R_2(\sigma) &= (-\mu - \gamma)\mu \\ Q_2(\sigma) &= (-\mu - \gamma)\sigma \end{aligned}$$

We square each of these equations.

$$\begin{aligned} R_1^2(\sigma) &= \sigma^4 - 2\mu\beta e^{-\mu\tau}\sigma^2 + \mu^2(\beta e^{-\mu\tau})^2 \\ Q_1^2(\sigma) &= ((\mu + \gamma)^2 + 2(\mu + \gamma)\mu R_0^{delay} + \mu^2(R_0^{delay})^2)\sigma^2 \\ R_2^2(\sigma) &= (\mu + \gamma)^2\mu^2 \\ Q_2^2(\sigma) &= (\mu + \gamma)^2\sigma^2 \end{aligned}$$

Then

$$\begin{aligned} S(z) = z^2 - \left(2\mu\beta e^{-\mu\tau} - (\mu + \gamma)^2 - 2(\mu + \gamma)\mu R_0^{delay} - \mu^2(R_0^{delay})^2 + (\mu + \gamma)^2 \right) z \\ + \mu^2(\beta e^{-\mu\tau})^2 - (\mu + \gamma)^2\mu^2 = 0 \end{aligned} \quad (3.15)$$

Algebraically, $S(z)$ is the quadratic equation. Note that $\sigma \in \mathbb{R}$. Suppose that z_1 and z_2 are the real roots of this equation. Then

$$\begin{aligned} (z - z_1)(z - z_2) &= 0 \\ z^2 - (z_1 + z_2)z + z_1z_2 &= 0 \end{aligned}$$

Case 1: if z_1z_2 is positive. Then z_1 and z_2 have to have the same sign. Therefore, if $z_1 + z_2$ is positive, then we can conclude that z_1 and z_2 are both positive. Otherwise, z_1 and z_2 are both negative.

Case 2: if z_1z_2 is negative. Then z_1 and z_2 have to have the different sign.

Case 3: if z_1z_2 is zero. Then one of the root has to be zero. Another one will have the sign as same as $z_1 + z_2$.

Back to our $S(z)$ equation. We have

$$\begin{aligned} z_1z_2 &= \mu^2(\beta e^{-\mu\tau})^2 - (\mu + \gamma)^2\mu^2 \\ z_1 + z_2 &= 2\mu\beta e^{-\mu\tau} - (\mu + \gamma)^2 - 2(\mu + \gamma)\mu R_0^{delay} - \mu^2(R_0^{delay})^2 + (\mu + \gamma)^2 \end{aligned}$$

Consider $z_1 z_2$,

$$\begin{aligned}
\mu^2(\beta e^{-\mu\tau})^2 - (\mu + \gamma)^2 \mu^2 &= \mu^2(\mu + \gamma)^2 \left(\frac{(\beta e^{-\mu\tau})^2}{(\mu + \gamma)^2} - 1 \right) \\
&= \mu^2(\mu + \gamma)^2 \left((R_0^{delay})^2 - 1 \right) \\
&> 0 \\
&\text{(Since } R_0^{delay} \text{ is greater than 1)}
\end{aligned}$$

Therefore, we are in case 1. So the roots have the same sign. We have to consider $z_1 + z_2$.

$$\begin{aligned}
z_1 + z_2 &= 2\mu\beta e^{-\mu\tau} - (\mu + \gamma)^2 - 2(\mu + \gamma)\mu R_0^{delay} - \mu^2(R_0^{delay})^2 + (\mu + \gamma)^2 \\
&= 2\mu\beta e^{-\mu\tau} - 2(\mu + \gamma)\mu R_0^{delay} - \mu^2(R_0^{delay})^2 \\
&= 2\mu\beta e^{-\mu\tau} - 2(\mu + \gamma)\mu \frac{\beta e^{-\mu\tau}}{\mu + \gamma} - \mu^2(R_0^{delay})^2 \\
&= -\mu^2(R_0^{delay})^2 \\
&< 0
\end{aligned}$$

Since $z_1 + z_2$ is negative, both z_1 and z_2 are negative.

But we know that z is σ^2 where $\sigma \in \mathbb{R}$. As a result, there is no such a σ^2 that satisfies negative number. This contradiction makes the claim that $\lambda = i\sigma$ being false. It implies that no λ changes from having negative real part to having positive real part. Consequently, E_2 does not have the Hopf bifurcation as well.

From this stability analysis, we can conclude that SEIR model will stay stable for each steady-state. Therefore, changing the value of delay will not cause periodic solutions.

3.3 SIRS model with delay

Usually, in SIRS model without delay, a factor of population over time will become susceptible again. However, the delay has been introduced so that it uses a period of time for those people to become susceptible again. Therefore, we want to study and find the conditions of the delay value for steady-states of this model become periodic solutions.

3.3.1 Steady-state E_3

First of all, we will consider the stability of the first steady-state E_3 . This happens only when the reproductive number less than 1. We want to find the roots of its characteristic equation. If all of the roots consist of negative real part, the Hopf bifurcation will not exist regardless of the delay value. On the other hand, if it is possible to have a positive real part in a root, it has a critical delay such that steady-state E_3 changes from being stable to being unstable.

From equation 2.26,

$$(-\mu - \alpha e^{-\mu\omega} e^{-\lambda\omega} - \lambda)(\beta - \mu - \gamma - \lambda) = 0$$

There are many roots for this equation because it is transcendental. One of the roots must be $\beta - \mu - \gamma$ or can be seen as $(\mu + \gamma)(R_0 - 1)$. We know that R_0 has to be less than 1 in order for this steady-state to be stable at $\tau = 0$. It implies that a root is a negative real number.

The others roots can be obtained by solving the following equation:

$$\lambda = -\mu - \alpha e^{-\mu\omega} e^{-\lambda\omega}$$

To start with, we consider λ in a complex form, $a + ib$. Substitute this complex solution into the equation above.

$$\begin{aligned} a + ib &= -\mu - \alpha e^{-\mu\omega} e^{-a\omega} e^{-ib\omega} \\ &= -\mu - \alpha e^{-\mu\omega} e^{-a\omega} (\cos(b\omega) - i\sin(b\omega)) \end{aligned} \quad (3.16)$$

Therefore, we have a system of equations.

$$a = -\mu - \alpha e^{-\mu\omega} e^{-a\omega} \cos(b\omega) \quad (3.17)$$

$$b = \alpha e^{-\mu\omega} e^{-a\omega} \sin(b\omega) \quad (3.18)$$

We want to find the critical delay in which the roots start to change from having negative real part to having positive real part. Therefore, we consider the solutions at imaginary axis by setting $a = 0$.

$$\begin{aligned} \mu &= -\alpha e^{-\mu\omega} \cos(b\omega) \\ b &= \alpha e^{-\mu\omega} \sin(b\omega) \end{aligned}$$

we sum the square of both equations.

$$\begin{aligned} b^2 + \mu^2 &= (\alpha e^{-\mu\omega})^2 (\cos^2(b\omega) + \sin^2(b\omega)) \\ b^2 &= (\alpha e^{-\mu\omega})^2 - \mu^2 \\ b &= \sqrt{(\alpha e^{-\mu\omega} - \mu)(\alpha e^{-\mu\omega} + \mu)} \end{aligned} \quad (3.19)$$

The purely imaginary root exists if and only if b is a real number. Therefore, $\alpha e^{-\mu\omega} - \mu$ has to be positive.

$$\begin{aligned} \alpha e^{-\mu\omega} &> \mu \\ e^{\mu\omega} &< \frac{\alpha}{\mu} \\ \omega &< \frac{\ln(\frac{\alpha}{\mu})}{\mu} \end{aligned} \quad (3.20)$$

Therefore, our critical delay ω^* is $\frac{\ln(\frac{\alpha}{\mu})}{\mu}$. To conclude, if the delay value less than ω^* , the steady-state E_3 can change from being stable to being unstable. If the delay value is large enough, the steady-state stays stable.

Note: This is different from other steady-states. As the delay decreases past the critical delay, the root will continue going into positive half-plane.

We use MATLAB to simulate the effect of the Hopf bifurcation. First of all, when the delay value is less than the critical delay, the solutions are stable as in figure 3.3. From figures 3.4, 3.5 and 3.6, the periodic solutions happen. Even though, it does not make sense for population to be negative or more than 10000 people (notice that that we have constant total population at 10000). In conclusion, the bifurcation happens when the delay value, ω , less than the critical delay, ω^* . The smaller delay is, the more swing occurs.

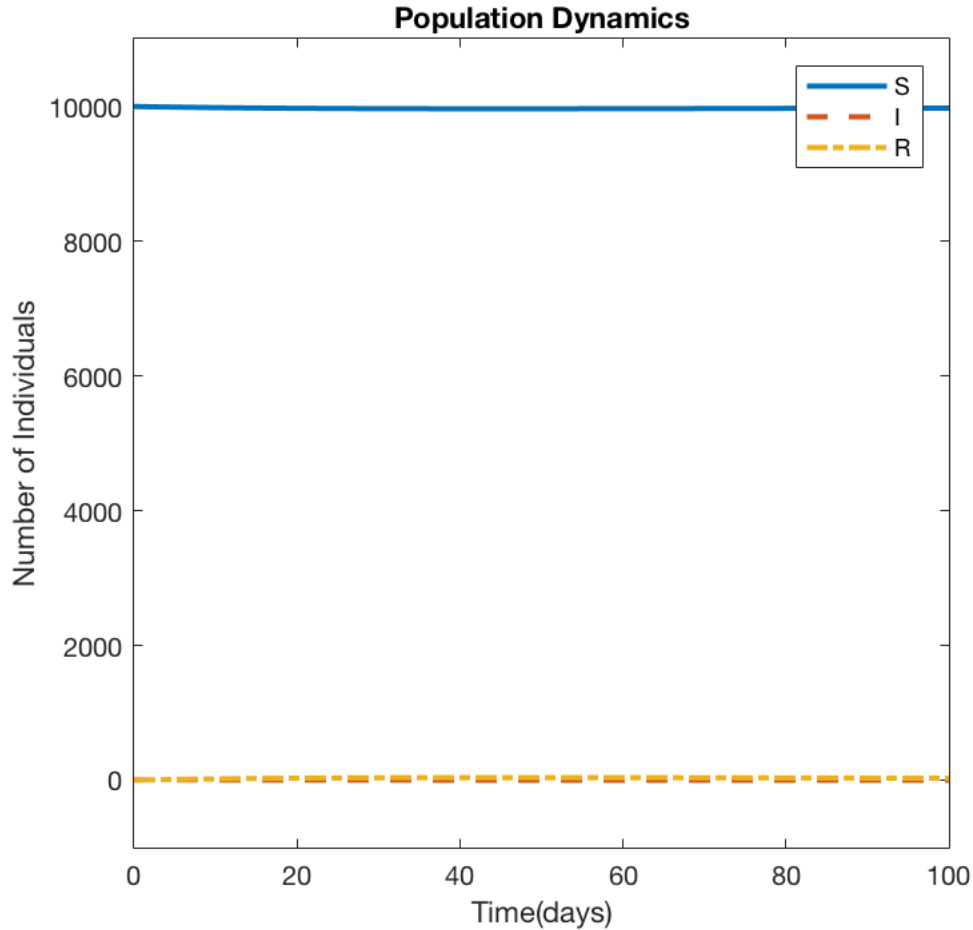


Figure 3.3: $\omega_1 > \omega^*$

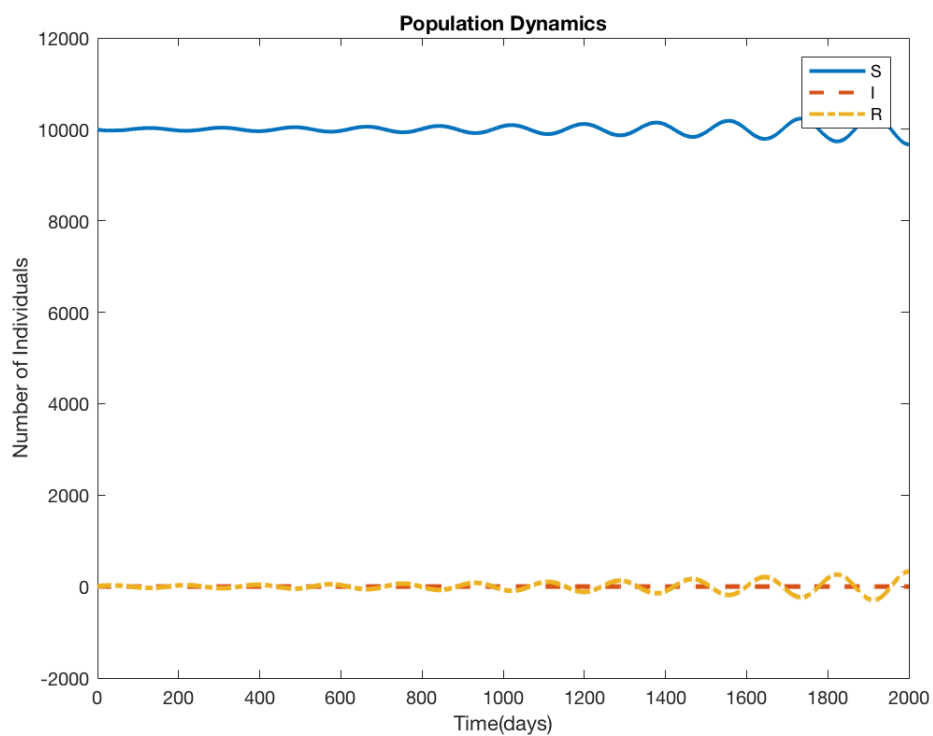


Figure 3.4: $\omega_1 = 80\%$ of ω^*

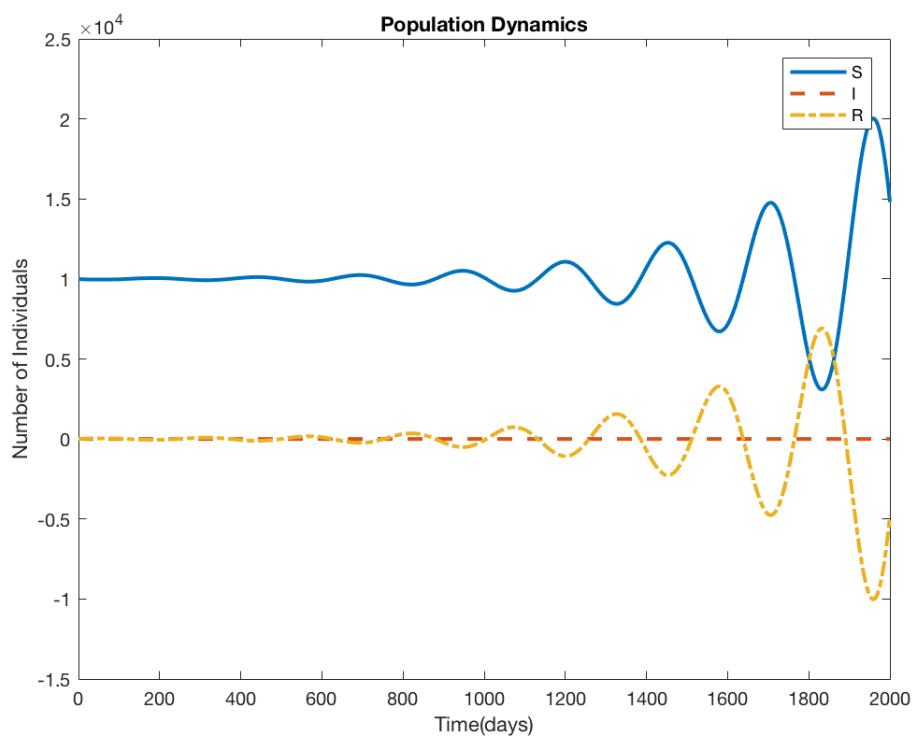


Figure 3.5: $\omega_1 = 70\%$ of ω^*

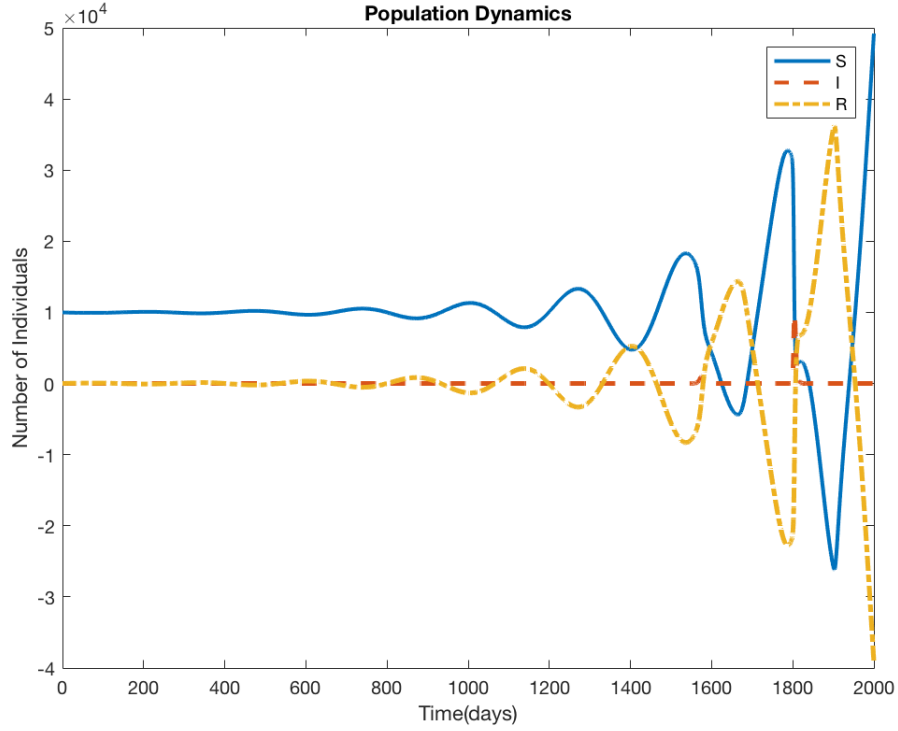


Figure 3.6: $\omega_1 = 60\%$ of ω^*

3.3.2 Steady-state E_4

For the steady-state E_4 , we also want to know at which ω^* that the eigenvalues change from having negative real part to having positive real part. So it is when the periodic solutions are going to emerge. We consider the characteristic for this steady-state.

$$P_{1,E_4}(\lambda) = \lambda^2 - (M - \mu)\lambda + \frac{\beta}{R_0}M$$

$$P_{2,E_4}(\lambda) = \alpha e^{-\mu\omega}\lambda + M\alpha e^{-\mu\omega}$$

where $M = \beta \frac{(R_0 - 1)(\mu + \alpha e^{-\mu\omega})}{(\beta + R_0 \alpha e^{-\mu\omega})}$. Then by using the tool 3.1, we can construct the following

$$R_1 = -\sigma^2 + \frac{\beta}{R_0}M$$

$$Q_1 = -(M - \mu)\sigma$$

$$R_2 = \mu\alpha e^{-\mu\omega}$$

$$Q_2 = \alpha e^{-\mu\omega}\sigma$$

Therefore, from equation 3.8, we have

$$\begin{aligned}
S(z) &= z^2 - 2\frac{\beta}{R_0}Mz + (\frac{\beta}{R_0}M)^2 + (M - \mu)^2z - (\mu\alpha e^{-\mu\omega})^2 - (\alpha e^{-\mu\omega})^2z \\
&= z^2 + Bz + C \\
&= 0
\end{aligned}$$

where

$$\begin{aligned}
B &= -2\frac{\beta}{R_0}M + (M - \mu)^2 - (\alpha e^{-\mu\omega})^2 \\
C &= (\frac{\beta}{R_0}M)^2 - (\mu\alpha e^{-\mu\omega})^2
\end{aligned}$$

Since $S(z)$ is a quadratic equation, the roots of this equation are

$$z = \frac{-B \pm \sqrt{B^2 - 4C}}{2}$$

Remember that z is σ^2 . In other word, z will exist if and only if it is a positive real number. If there is no such z , then there is no eigenvalue that has purely imaginary part and the Hopf bifurcation does not happen.

Let $z^* \in z$. Suppose that z^* is a positive real roots. Then $\sigma^* = \pm\sqrt{z^*}$, and we can substitute this σ^* into equations 3.3 and 3.4.

$$\begin{aligned}
-R_1(\sigma^*) &= R_2(\sigma^*)\cos(\sigma^*\omega) + Q_2(\sigma^*)\sin(\sigma^*\omega) \\
Q_1(\sigma^*) &= R_2(\sigma^*)\sin(\sigma^*\omega) - Q_2(\sigma^*)\cos(\sigma^*\omega)
\end{aligned}$$

Consequently the two equations contain only ω variable. Therefore, we can find ω^* that satisfy the two equations. Remember that if we have more than one ω^* 's, we will choose the smallest positive one; any ω that is greater than the smallest critical delay is going to cause the Hopf bifurcation in the solutions.

However, finding the critical delay for this steady-state algebraically is difficult. Thus, we will use MATLAB to approximate the solution numerically. First, we find the positive real number z^* , and then use *fsolve* in MATLAB to approximate the critical delay. After we have that ω^* , we vary ω around ω^* to show the Hopf bifurcation. Moreover, we are going to study the effect of the reproductive number on this bifurcation. The results are the following:

Considering different values of delay ω based on the critical delay, ω^*

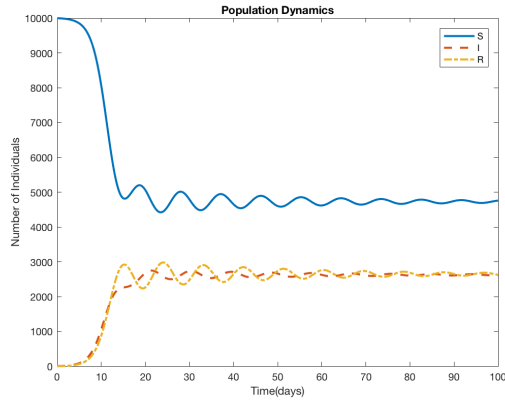


Figure 3.7: $\omega = \omega^*$

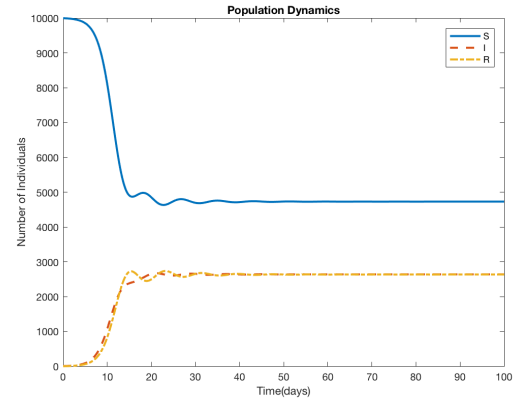


Figure 3.8: $\omega = \omega^* - 0.1$

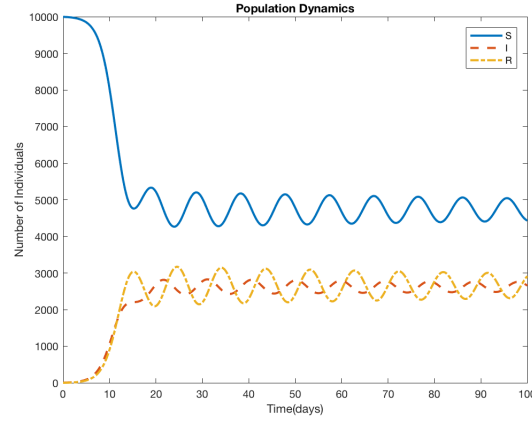


Figure 3.9: $\omega = \omega^* + 0.1$

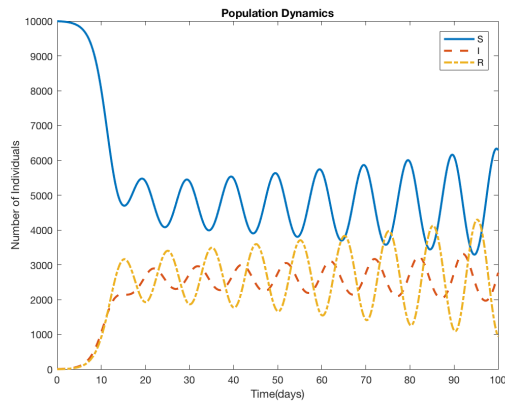


Figure 3.10: $\omega = \omega^* + 0.2$

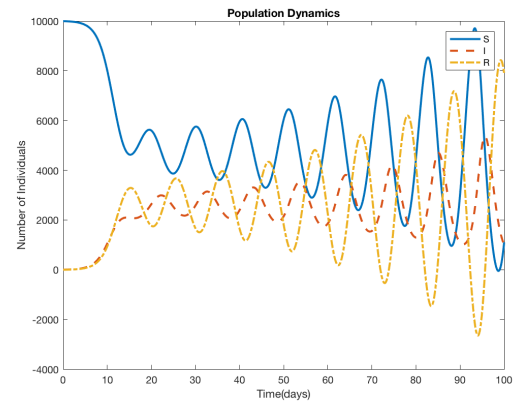


Figure 3.11: $\omega = \omega^* + 0.3$

Considering different reproductive numbers when $\omega = 2\omega^*$

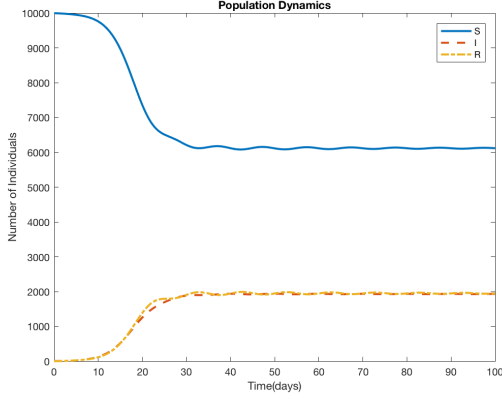


Figure 3.12: $R_0 = 1.6346$

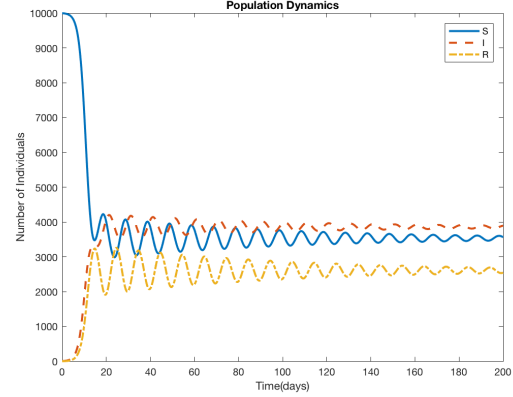


Figure 3.13: $R_0 = 2.8302$

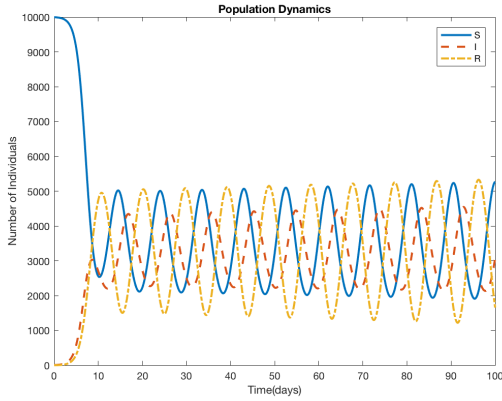


Figure 3.14: $R_0 = 2.8846$

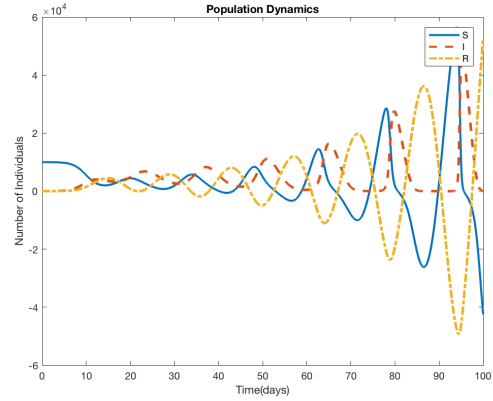


Figure 3.15: $R_0 = 3.7037$

In conclusion, steady-state E_4 always has the critical value so that the eigenvalues change from having negative real part to having positive real part; when the delay ω is less than the critical delay ω^* , there will be no oscillation at the steady-state E_4 , figure 3.8; when we increase the ω to be equal to ω^* , figure 3.7, the Hopf bifurcation starts to happen. Once we choose ω to be 0.1 larger than ω^* in figure 3.9, we clearly see more of periodic solutions. We can keep increasing the delay and the oscillation will keep becoming bigger, shown in figures 3.10 and 3.11. Notice that the periodic solutions will oscillate on a line which, in fact, is where the steady-state E_4 lines on. In figure 3.10 and 3.11, ω is large enough to make the oscillation keeps larger when time increases. So the severe outbreaks will happen in this case. Additionally, when R_0 increases and the size of ω is fixed to be two times of ω^* , the oscillation apparently increases its amplitude over time.

In summary, for both steady-states of this SIRS model, the Hopf bifurcation happens. Steady-state E_3 changes from being stable to being unstable when the delay less than its critical delay. However, the results calculated from MATLAB show that the critical delay is going to be bigger than the life-cycle μ . Therefore, we can conclude that the oscillation

always happen in if the steady-state E_3 exists. For steady-state E_4 , the periodic solutions definitely occurs when ω is greater than ω^* . In addition to the value of delay, R_0 affects the oscillation as well. The larger R_0 is, the stronger oscillations swings.

3.4 Chemostat model with delay

There are two steady-states for this chemostat model. We will consider their stability while changing the delay ω .

3.4.1 Steady-state F_1

Steady-state F_1 is the case when the rate of growth is less than the flow rate of the tank. Thus, the number of cells will go to zero. In our study, we want to know if we change the value of delay, how it affects the behavior of the solutions.

To understand this phenomenon, we consider the characteristic equation 2.37.

$$\lambda^2 + 2\lambda + 1 + \left(-\frac{\gamma\beta e^{-\omega}}{1+\gamma}\lambda - \frac{\gamma\beta e^{-\omega}}{1+\gamma} \right) e^{-\lambda\omega} = 0$$

Without delay, or $\omega = 0$, this characteristic equation becomes

$$\lambda^2 + 2\lambda + 1 + \left(-\frac{\gamma\beta e^{-\omega}}{1+\gamma}\lambda - \frac{\gamma\beta e^{-\omega}}{1+\gamma} \right).$$

Remember that $R_0 < 1$ for this steady-state F_1 :

$$\begin{aligned} & \gamma(\beta e^{-\omega} - 1) < 1 \\ \Leftrightarrow & \gamma\beta e^{-\omega} < 1 + \gamma \\ \Leftrightarrow & \frac{\gamma\beta e^{-\omega}}{1 + \gamma} < 1 \end{aligned}$$

Therefore, all of the eigenvalues when $\omega = 0$ have negative real part. Therefore, it is stable.

Using strategy 3.1, we have

$$\begin{aligned} R_1(\sigma) &= -\sigma^2 + 1 \\ Q_1(\sigma) &= 2\sigma \\ R_2(\sigma) &= -M \\ Q_2(\sigma) &= -M\sigma \end{aligned}$$

where $M = \frac{\gamma\beta e^{-\omega}}{1 + \gamma} < 1$.

Then, we construct $S(z)$ as in 3.8.

$$\begin{aligned} S(z) &= z^2 - 2z + 1 + 4z - M^2 - M^2z \\ &= z^2 - (-2 + M^2)z + 1 - M^2 = 0 \end{aligned}$$

Suppose that roots of this equation are z_1 and z_2 .

$$z_1 z_2 = 1 - M^2 \quad (3.21)$$

$$z_1 + z_2 = -2 + M^2 \quad (3.22)$$

Since $M < 1$, M^2 is definitely less than 1 and 2. We know that z_1 and z_2 have to be negative numbers in order for 3.21 and 3.22 being satisfied. Hence, there is not a Hopf bifurcation for steady-state F_1 . F_1 stays stable.

In conclusion, sometimes we want to drive the population of a cell to zero. Then we do not need to worry about the time delay of growing of this cell; The delay will not change the stability of this situation (in the condition that $R_0 < 1$).

3.4.2 Steady-state F_2

This is the situation when the cell will stay at the same population size when the time goes to infinity as well as the concentration of the nutrient. We will analyze its stability by using the tool 3.1. Remember that R_0 greater than 1 in this case.

Consider the characteristic equation 2.38

$$P_{F_2}(\lambda, \tau) = \lambda^2 + \left(2 + \frac{R_0 - 1}{H}\right) \lambda + 1 + \frac{R_0 - 1}{H} + \left(-\beta e^{-\omega} \left(1 - \frac{1}{H}\right) (\lambda + 1)\right) e^{-\lambda \omega}$$

$$R_1 = -\sigma^2 + N$$

$$Q_1 = (1 + N) \sigma$$

$$R_2 = -L$$

$$Q_2 = -L\sigma$$

where $N = 1 + \frac{R_0 - 1}{H}$ and $L = \beta e^{-\omega} \left(1 - \frac{1}{H}\right)$.

Rewrite L by back-substituting $H = 1 + \frac{1}{\beta e^{-\omega} - 1} = \frac{\beta e^{-\omega}}{\beta e^{-\omega} - 1}$.

$$\begin{aligned} L &= \beta e^{-\omega} \left(\frac{H - 1}{H} \right) \\ &= \beta e^{-\omega} \left(\frac{\frac{1}{\beta e^{-\omega} - 1}}{\frac{\beta e^{-\omega}}{\beta e^{-\omega} - 1}} \right) \\ &= 1 \end{aligned}$$

Following the step in the introduction part of this chapter, we have

$$R_1^2 = \sigma^4 - 2N\sigma^2 + N^2$$

$$Q_1^2 = (1 + 2N + N^2) \sigma^2$$

$$R_2^2 = 1$$

$$Q_2^2 = \sigma^2$$

Then

$$\begin{aligned} S(z) &= z^2 - (2N - 1 - 2N - N^2 + 1)z + N^2 - 1 \\ &= z^2 - (-N^2)z + N^2 - 1 \\ &= 0 \end{aligned}$$

We know that $N > 1$. So it is obviously that the solutions of this equation are both negative real number. In the other word, the stability of this steady-state F_2 with the $\omega = 0$ will not change from being stable to being unstable while increasing ω .

After consuming the nutrient, some cells might develop to have faster or slower delay time to grow. Fortunately, if the cells satisfy this model, when R_0 is greater than 1, the delay value will no affect the stability of the solutions. Without the solution of this steady-state, we will still be concerned about it when we want to keep the population dynamic of the cells beyond zero.

In conclusion, for chemostat model, the steady-states F_1 and F_2 stay stable regardless of the value of the delay ω .

Chapter 4

Global Sensitivity Analysis

Human susceptibility, virus nature, climate and transmission rates can change for both the SIR and the Chemostat model. In order to understand how this variation could affect our outputs, we quantify the impact of changes in parameters. Sensitivity analysis is a study of how uncertainty in the output of a model can be attributed to different sources of uncertainty in the model input. For the software we use in this research, MatLab, sensitivity analysis refers to understanding how the parameters and steady states of a model influence the characteristic function. There are several different sensitivity analysis methods, such as local sensitivity analysis, Extended Sensitivity Analysis and global sensitivity analysis.

Local Sensitivity Analysis: Local sensitivity analysis works for at particular parameter values assuming that all other parameters are fixed.

Extended Sensitivity Analysis: Extended sensitivity analysis calculates the response of the model to variations in each parameter of interest over its range of possible values, while fixing all of the other parameters at their baseline values.

Global Sensitivity Analysis: The global sensitivity analysis varies one parameter at a time, but still only samples a very small region in the space of possible parameter values.

Local sensitivity analysis and extended sensitivity focus on the effect of one parameter on the function at a time, keeping the other parameters fixed. They can only explore a small

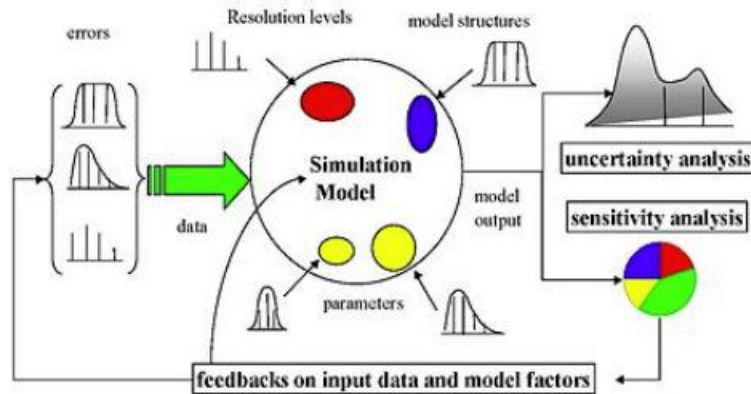


Figure 4.1: The Process of Global Sensitivity Analysis

fraction of the design space, especially when there are many parameters. They do not provide insight about how the interactions between parameters influence the function. In this case, we mainly use global sensitivity analysis in our research. The global sensitivity analysis uses a global set of samples to explore the design space. Fig. 4 shows the process of global sensitivity analysis.

Before we do the global sensitivity analysis, we separate all the parameters into two groups: parameters of interest (POI) and quantities of interest (QOI). We have three types parameters of interest (POI) in each model. They are the parameters we can control, the ones we only know approximately, and the parameters that cannot be defined to be a specific value because of random stochastic effects. The usefulness of a model depends on understanding the uncertainties in our parameters affect predictions of quantities of interest (QOI). Usually, we can get the response of the QOI to POI that we could control.

We are going to first introduce the main method which we used for analyzing all the models, then explain the details for the difference between different quantities of interest (QOI) in each sub-sections.

There are different possibilities in parameter values depending on environment, climate, peoples behavior, so we computed distributions for each of the QOI while varying all parameters across their ranges simultaneously. The method we used can be found in Appendix B in this paper [11]. We start by describing POI $p = (p_1, p_2, \dots, p_n) \in R^n$ satisfies, $p_i \in [p_i^-, p_i^+]$ for $i=1,2,\dots,n$. For each POI and QOI, we also give them a baseline value. (We use the notation $\hat{\cdot}$ to indicate that a variable is evaluated at the model baseline values.) We sample in this feasibility space N times using Sobol sampling, yielding $p^j = (p_1^j, p_2^j, \dots, p_n^j)$, $j = 1, \dots, M$. We solve the model for each p^j to generate the corresponding QOI, q^j . To form a distribution of the QOI from these samples we use a kernel density estimate (KDE) where the estimate of the probability density function for q_i is given by

$$\hat{f}_h(q_i) = \frac{1}{Mh} \sum_{j=1}^M K\left(\frac{q_i - q_i^j}{h}\right)$$

Here N is the iteration time which the number of calculating time we want for each QOI. In our paper, we use $M = 5000$ for each QOI. $K(u)$ is a compactly supported function on R and $h > 0$ is the bandwidth of the KDE. For our research, we take $K(u)$ to be the Epanechnikov kernel

$$K(u) = \frac{3}{4}(1 - u^2)I_{|u| \leq 1}$$

The bandwidth $h > 0$ is chosen so that $\hat{f}_h(q)$ is sufficiently regularized to show the shape of the distribution. In our paper, we change h depend on different parameter. We will note h in each sub-sections. Distributions and sensitivity for all quantities of interest (QOI) are shown in the following subsections.

Since our models are generated form the original model depends on the time delay, we use a dde23 in MatLab for solving the delay equations by choosing tspan (the interval of integration) between 0 and 30 for all models we analyze.

4.1 The SEIR model with Incubation Period

From Chapter 2, we have the delay equations for the SEIR model.

$$\begin{aligned}\frac{dS(t)}{dt} &= \mu N(t) - \frac{\beta S(t)I(t)}{N(t)} - \mu S(t) \\ \frac{dE(t)}{dt} &= \frac{\beta S(t)I(t)}{N(t)} - \frac{\beta S(t-\tau)I(t-\tau)}{N(t)} e^{-\mu\tau} - \mu E(t) \\ \frac{dI(t)}{dt} &= \frac{\beta S(t-\tau)I(t-\tau)}{N(t)} e^{-\mu\tau} - \gamma I(t) - \mu I(t) \\ \frac{dR(t)}{dt} &= \gamma I(t) - \mu R(t)\end{aligned}$$

In our analysis, we assumed that each of the POIs are changing independently of each other. If the POIs are related, then this must be taken into account in the sampling algorithm. We assumed uniform distributions for the parameter ranges. If more information is known about these distributions, then the sampling can reflect the known distribution. For the SEIR model with incubation period, we consider all the variables listed in table4.1 as POIs. The solution of the mathematical models for the base line parameters, shown in table4.2. The birth and death rate never change in our model, and we assumed the total number of people in the SIR model is 10000. These two fixed parameters shown in table4.3. Since POI is only known approximately, it can be difficult to quantify the full range of possible model predictions.

Table 4.1: Parameters of interest(POI) for the SEIR Model

β	Transmission probability: uniformly chosen in (0.4, 2)
γ	Recovery rate: uniformly chosen in (1/2, 1/7)
τ	Time delays: uniformly chosen in (0, 10)

Table 4.2: Quantities of interest(QOI) for the SEIR Model

$I(t)$	The maximum number of infected people during the whole infection process.
$t(I)$	The time to reach the maximum number of infected people during the whole infection process.
$\int_0^T I(t)dt$	The number of all people got infected during the whole infection process.

By tabulating all of the sample responses for a single QOI, we can create the one-dimensional distribution for the QOI. This simple approach provides a quick analyze of the

Table 4.3: Fixed parameters for the SEIR Model

μ	The birth rate and death rate: chosen as $1/100$
N	The total number of the whole balance for SIR model as $S + I + R = N$: chosen as $N = 10000$

possible range of QOI within the parameter ranges and indicates the frequency with which QOI values will occur. For each QOI, we analyze the global sensitivity of our three different POI, by fixing other two of them at the baseline values and random the one we focus on.

4.1.1 Global Sensitivity Analysis with Peak of $I(t)$

In order to analyze the global sensitivity of peak of $I(t)$, we analyzed three times each for β, γ and τ . We choose $M = 5000$.

For β , fix $\gamma = 1/6$, $\tau = 5$, $h = 50$ and uniformly β in $(0.4, 2)$. The distribution shows in figure4.2.

For γ , fix $\beta = 1$, $\tau = 5$, $h = 400$ and uniformly γ in $(1/2, 1/7)$. The distribution shows in figure4.3.

For τ , we fix $\gamma = 1/6$, $\beta = 1$, $h = 50$ and uniformly τ in $(0, 10)$. The distribution shows in figure4.4.

By looking at how fat of the curves are, we can tell that for QOI: peak of $I(t)$, β and τ are the most sensitive parameters.

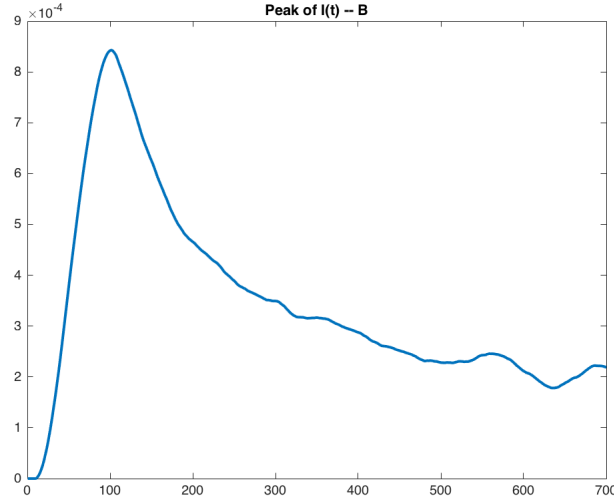


Figure 4.2: $Peak - I(t) - \beta \in (0.4, 2)$, $\gamma = 1/6$, $\tau = 5$, $h = 50$

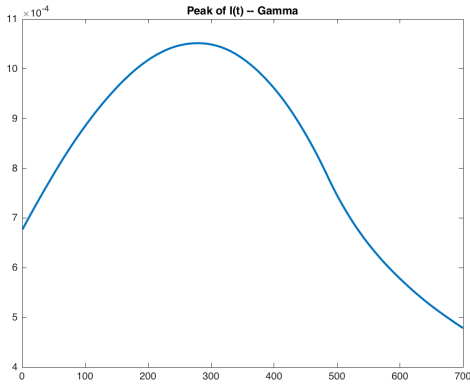


Figure 4.3: $Peak - I(t) - \gamma \in (1/2, 1/7)$, $\beta = 1$, $\tau = 5$, $h = 400$

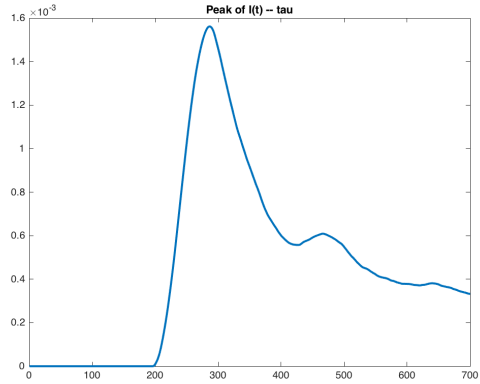


Figure 4.4: $Peak - I(t) - \tau \in (0, 10)$, $\gamma = 1/6$, $\beta = 1$, $h = 50$

4.1.2 Global Sensitivity Analysis with $t(I)$

In order to analyze the global sensitivity of $t(I)$, we analyzed three times each for β, γ and τ . We choose $M = 5000$ and $h = 50$ for each parameter.

For β , fix $\gamma = 1/4$, $\tau = 5$, and uniformly β in $(0.4, 2)$. The distribution shows in 4.5.

For γ , fix $\beta = 1$, $\tau = 5$, and uniformly γ in $(1/2, 1/7)$. The distribution shows in 4.6.

For τ , fix $\beta = 1$, $\gamma = 1/4$, and uniformly τ in $(0, 10)$. The distribution shows in 4.7.

By looking at how fat of the curves are, we can tell that for QOI: $t(I)$, all the three POI are equally sensitive.

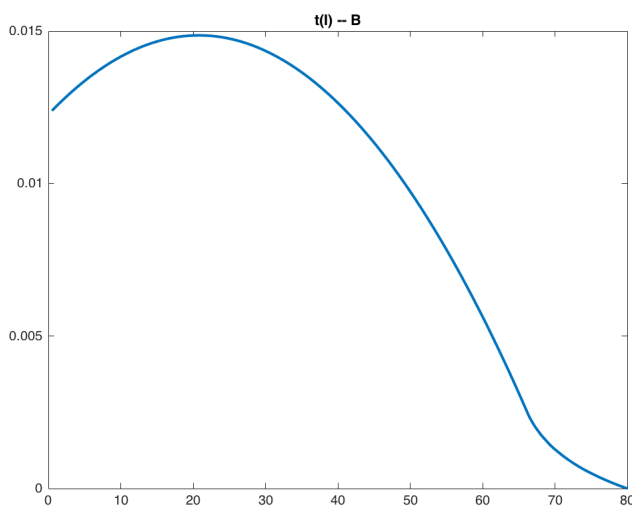


Figure 4.5: $t(I) - \beta \in (0.4, 2)$, $\gamma = 1/4$, $\tau = 5$

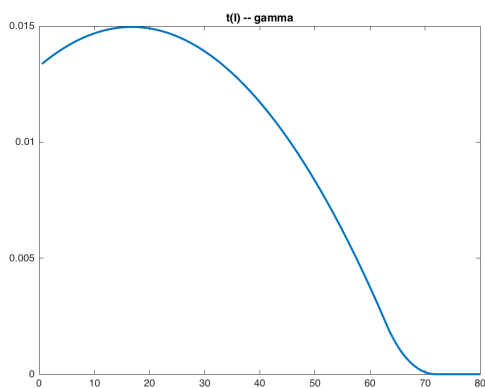


Figure 4.6: $t(I) - \gamma \in (1/2, 1/7)$, $\beta = 1$, $\tau = 5$

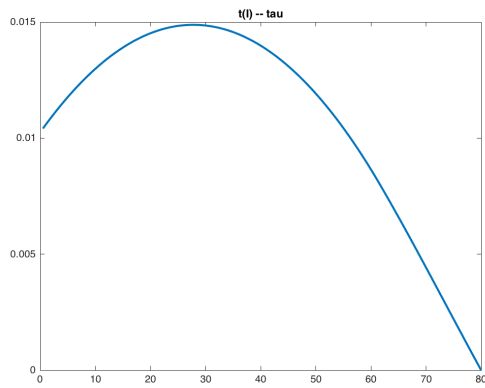


Figure 4.7: $t(I) - \tau \in (0, 10)$, $\beta = 1$, $\gamma = 1/4$

4.1.3 Global Sensitivity Analysis with $\int_0^T I(t)dt$

In order to analyze the global sensitivity of integral of $I(t)$, we analyzed three times each for β, γ and τ . We choose $M = 5000$.

For β , fix $\gamma = 1/4$, $\tau = 5$, $h = 1000$ and uniformly β in $(0.4, 2)$. The distribution shows in 4.8.

For γ , fix $\beta = 1$, $\tau = 5$, $h = 1000$ and uniformly γ in $(1/2, 1/7)$. The distribution shows in 4.9.

For τ , fix $\gamma = 1/4$, $\beta = 1$, $h = 1000$ and uniformly τ in $(0, 10)$. The distribution shows in 4.10.

By looking at how fat of the curves are, we can tell that for QOI: $\int_0^T I(t)dt$, β and τ are the most sensitive parameters.

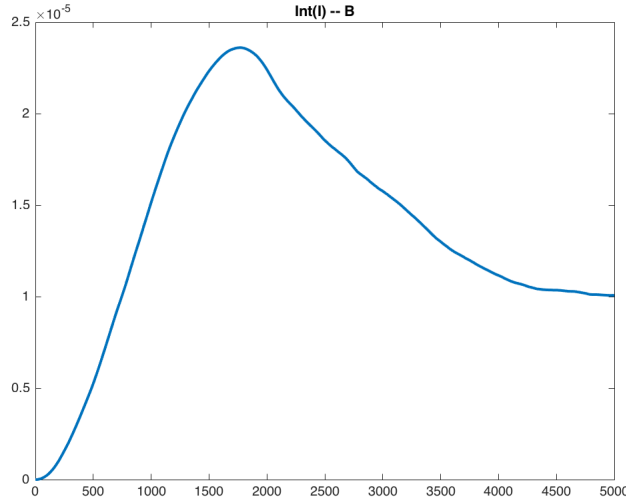


Figure 4.8: $\int_0^T I(t)dt - \beta \in (0.4, 2)$, $\gamma = 1/4$, $\tau = 5$, $h = 1000$

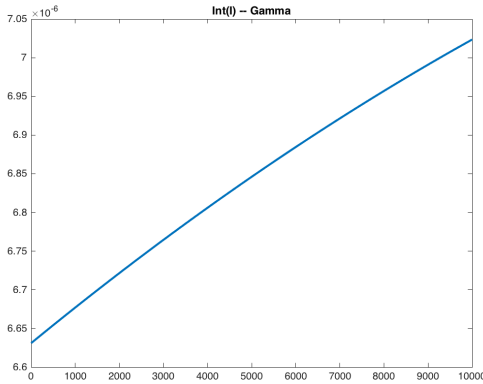


Figure 4.9: $\int_0^T I(t)dt - \gamma \in (1/2, 1/7)$, $\beta = 1$, $\tau = 5$, $h = 1000$

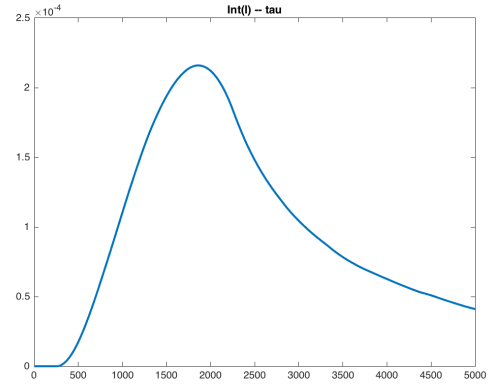


Figure 4.10: $\int_0^T I(t)dt - \tau \in (0, 10)$, $\gamma = 1/4$, $\beta = 1$, $h = 1000$

4.2 The Chemostat

From Chapter 2, we have the delay equations for the chemostat model.

$$\begin{aligned}\frac{dX}{dt} &= e^{-\omega \frac{K_1}{F}} \frac{Y(t-\omega)X(t-\omega)}{1+Y(t-\omega)} - X \\ \frac{dY}{dt} &= \frac{N_0}{K_2} - Y(t) - \frac{Y(t)X(t)}{1+Y(t)}\end{aligned}$$

For the chemostat model with time delay, we consider all the variables listed in table 4.4 as POIs. The solution of the mathematical models for the base line parameters, shown in table 4.5. Since POI is only known approximately, it can be difficult to quantify the full range of possible model predictions.

Table 4.4: Parameters of interest(POI) for the Chemostat Model

K_1	Maximum growth rate: uniformly chosen in (0.1, 1)
K_2	Nutrient concentration calculated at 1/2 the maximum growth rate: uniformly chosen in (0.01, 0.1)
ω	The cell uses ω time to grow after consume the nutrient: uniformly chosen in (0.1, 1.2)

Table 4.5: Quantities of interest(QOI) for the Chemostat Model

$\int_0^T X(t)dt$	The number of cell in this experiment.
-------------------	--

By tabulating all of the sample responses for a single QOI, we can create the one-dimensional distribution for the QOI. This simple approach provides a quick analyze of the possible range of QOI within the parameter ranges and indicates the frequency with which QOI values will occur. For each QOI, we analyze the global sensitivity of our three different POI, by fixing other two of them at the baseline values and random the one we focus on.

4.2.1 Global Sensitivity Analysis with $\int_0^T X(t)dt$

In order to analyze the global sensitivity of integral of $X(t)$, we analyzed three times each for K_1, K_2 and ω . We choose $M = 5000$ and $h = 50$.

For K_1 , fix $K_2 = 0.0727$, $\omega = 1.1$, and uniformly K_1 in $(0.1, 1)$. The distribution shows in 4.11.

For K_2 , fix $K_1 = 0.7726$, $\omega = 1.1$, and uniformly K_2 in $(0.01, 0.1)$. The distribution shows in 4.12.

For ω , fix $K_1 = 0.7726$, $K_2 = 0.0727$, and uniformly ω in $(0.1, 1.2)$. The distribution shows in 4.13.

The three graphs imply that the three POIs have the same affect on this QOI.

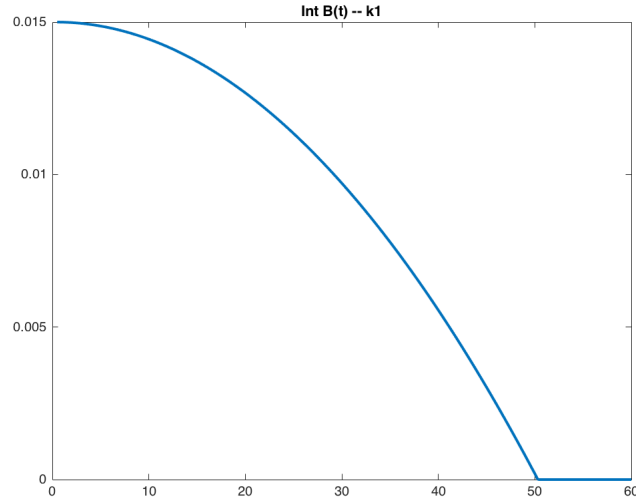


Figure 4.11: $\int_0^T X(t)dt - K_1 \in (0.1, 1)$, $K_2 = 0.0727$, $\omega = 1.1$

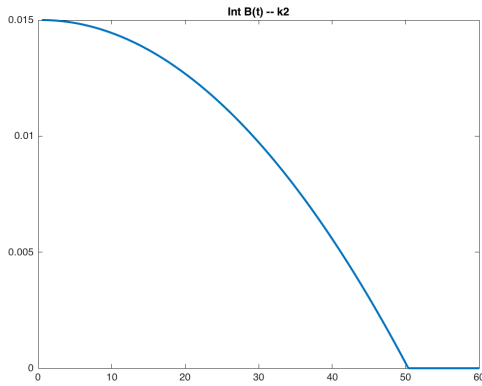


Figure 4.12: $\int_0^T X(t)dt - K_2 \in (0.01, 0.1)$, $K_1 = 0.7726$, $\omega = 1.1$

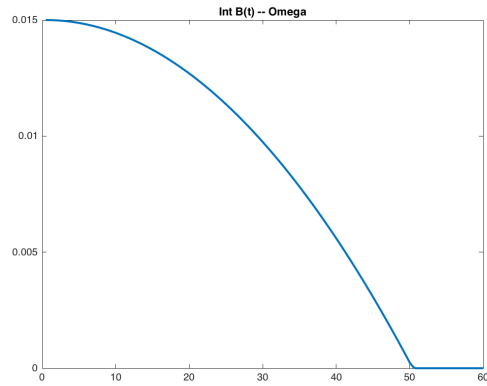


Figure 4.13: $\int_0^T X(t)dt - \omega \in (0.1, 1.2)$, $K_1 = 0.7726$, $K_2 = 0.0727$

Chapter 5

Conclusion

This Major Qualifying Project can be divided into three main chapters. For each chapter, we studied three different biological mathematical models with time delay, which are the Logistic Growth model, the SIR model and the Chemostat model.

In chapter two and chapter three, we find out that for each model, there are two steady-states and based on the steady-state, we generated characteristic equation. We also analyze the stability of steady-states of all the model. The Hopf bifurcation occurs in the logistic growth model and the SIRS model with delay, but not in the SEIR model with delay and the chemostat model. During our study of the logistic growth model and the SIRS model with delay, we have the following results:

For the logistic growth model, the steady-state D_1 is always unstable since we only get positive real root by solving the characteristic equation. However, at steady-state D_2 , the Hopf bifurcation occurs when the delay is greater than critical value $\frac{\pi}{2r}$.

For the SIRS model with delay, Hopf bifurcation behaves differently for each steady-state. At steady-state E_3 , periodic solutions occur when the delay is less than critical value $\frac{\ln(\frac{\alpha}{\mu})}{\mu}$. This critical value is usually greater than the value of lifespan $\frac{1}{\mu}$. We know that the delay should be less than $\frac{1}{\mu}$, so it implies that Hopf bifurcation always happens in this case. On the other hand, the oscillation of steady-state E_4 occurs when the delay is greater than the critical delay. It is difficult to find the explicit form of this critical delay algebraically. Instead, we use MATLAB numerical approximation to calculate this value.

In chapter four, we study global sensitivity analysis for the SEIR model with delay and the chemostat model. We first analyze the POI and QOI for each model. Then we use 'dde23' in MATLAB for solving the delay equations. By tabulating all of the sample responses for a single QOI, we can create the one-dimensional distribution for the QOI by using the KDE function. For each QOI, we analyze the global sensitivity of three different POIs, by fixing two of them at the baseline values and randomize the one we focus on. This simple approach provides a quick analyze of QOI within the value range and indicates relations with all the POI.

Appendix A

MATLAB Code

This is one example MatLab code of solving the peak of $I(t)$ with parameter β . For other QOI, we use the same method with changing parameters and their baseline value.

```
1 %%%%%%%%%%%%%%%%%%%%%%%%%%%%%%%%%%%%%%%%%%%%%%%%%%%%%%%%%%%%%%%%%%%%%%%%%%
2 %%%%%%%%%%%%%%%%%%%%%%%%%%%%%%%%%%%%%%%%%%%%%%%%%%%%%%%%%%%%%%%%%%%%%%%%%%I ( t )-B%%%%%%%%%%%%%%%%%%%%%%%%%%%%%%%%%%%%%%%%%%%%%%%%%%%%%%%%%%%%%%%%%%%%%%%%%
3 %%%%%%%%%%%%%%%%%%%%%%%%%%%%%%%%%%%%%%%%%%%%%%%%%%%%%%%%%%%%%%%%%%%%%%%%%%
4 function [x,sum,tau,I] = MQP_I_t_B(maxiteri)
5 global tau
6 global gamma
7 global miu
8 global maxiter
9 global B
10 global N
11 %miu = 1/(78*365);
12 miu = 1/100;
13
14 %B = randnum(0.4,2);
15 %gamma = randnum(2,7);
16 tau = 5;
17 x=0.5:0.1:700;
18 %B = 1.0;
19 gamma = 1/6;
20 maxiter = maxiteri;
21 N=10000;
22 %h = 500;
23 h = 50;
24 tspan = 0:30;
25
26 for i=1:maxiter
27     %tau = randnum(2,7);    % a vector of tau
28     B = randnum(.4,2);
29     sol = dde23(@delay_func,tau,@history,tspan);
30     I(i) = max(sol.y(3,:)); % this is my QOI
```

```

31     %r = R0(B);
32 end
33 %[min(r),max(r)]
34 sum = zeros(1,length(x));
35
36 for ell=1:length(x)
37     % for each x(ell), sum over all QOI
38     %sum = zeros(1,length(x));
39     for k=1:maxiter
40         tmp(k) = (x(ell)-I(k))/h;
41         sum(ell) = sum(ell) + KDE(tmp(k));
42         KDE(tmp(k));
43     end
44     sum(ell) = sum(ell)/(maxiter*h);
45     % now you have (x,sum)
46 end % end ell loop
47
48 end

1  %%%%%%%%%%%%%%%%%%%%%%%%%%%%%%%%%%%%%%%%%%%%%%%%%%%%%%%%%%%%%%%%%%%%%%%%%%
2  %%%%%%%%%%%%%%%%%%%%%%%%%%%%%%%%%%%%%%%%%%%%%%%%%%%%%%%%%%%%%%%%%%%%%%%%%%delay function%%%%%%%%%%%%%%%%%%%%%%%%%%%%%%%%%%%%%%%%%%%%%%%%%%%%%%%%%%%%%%%%%%%%%%%%%
3  %%%%%%%%%%%%%%%%%%%%%%%%%%%%%%%%%%%%%%%%%%%%%%%%%%%%%%%%%%%%%%%%%%%%%%%%%%
4  function dydt = delay_func(t,y,Z)
5  ylag = Z(:,1);
6
7  global N
8  global tau
9  global gamma
10 global miu
11 global B
12
13 dydt = zeros(4,1);
14 dydt(1) = miu*N - B*y(1)*y(3)/N - miu*y(1);
15 dydt(2) = B*y(1)*y(3)/N - B*ylag(1)*ylag(3)/N*exp(-miu*tau) - miu*y
    (2);
16 dydt(3) = B*ylag(1)*ylag(3)/N*exp(-miu*tau) -gamma*y(3)- miu*y(3);
17 dydt(4) = gamma*y(3)-miu*y(4);
18
19 end

1  %%%%%%%%%%%%%%%%%%%%%%%%%%%%%%%%%%%%%%%%%%%%%%%%%%%%%%%%%%%%%%%%%%%%%%%%%%
2  %%%%%%%%%%%%%%%%%%%%%%%%%%%%%%%%%%%%%%%%%%%%%%%%%%%%%%%%%%%%%%%%%%%%%%%%%%history function%%%%%%%%%%%%%%%%%%%%%%%%%%%%%%%%%%%%%%%%%%%%%%%%%%%%%%%%%%%%%%%%%%%%%%%%%
3  %%%%%%%%%%%%%%%%%%%%%%%%%%%%%%%%%%%%%%%%%%%%%%%%%%%%%%%%%%%%%%%%%%%%%%%%%%
4  function y0 =history(t)
5  global N
6  % y0 = [S, E, I, R]

```

```

7  y0 = zeros(4,1);
8  y0(1,1) = N-5;
9  y0(2,1) = 0;
10 y0(3,1) = 5;
11 y0(4,1) = 0;
12
13 end

1  %%%%%%%%%%%%%%%%%%%%%%%%%%%%%%%%%%%%%%%%%%%%%%%%%%%%%%%%%%%%%%%%%%%%%%%%%%
2  %%%%%%%%%%%%%%%%%%%%%%%%%%%%%%%%%%%%%%%%%%%%%%%%%%%%%%%%%%%%%%%%%%%%%%%%%%KDE function%%%%%%%%%%%%%%%%%%%%%%%%%%%%%%%%%%%%%%%%%%%%%%%%%%%%%%%%%%%%%%%%%%%%%%%%%
3  %%%%%%%%%%%%%%%%%%%%%%%%%%%%%%%%%%%%%%%%%%%%%%%%%%%%%%%%%%%%%%%%%%%%%%%%%%
4  function f = KDE(z)
5  % z is a a vector
6  % returns the function (3/4)*(1-miu^2)*I{|miu\^2<1}
7  f = (3/4)*max(1-z^2,0);
8  end

1  %%%%%%%%%%%%%%%%%%%%%%%%%%%%%%%%%%%%%%%%%%%%%%%%%%%%%%%%%%%%%%%%%%%%%%%%%%
2  %%%%%%%%%%%%%%%%%%%%%%%%%%%%%%%%%%%%%%%%%%%%%%%%%%%%%%%%%%%%%%%%%%%%%%%%%%randnum function%%%%%%%%%%%%%%%%%%%%%%%%%%%%%%%%%%%%%%%%%%%%%%%%%%%%%%%%%%%%%%%%%%%%%%%%%
3  %%%%%%%%%%%%%%%%%%%%%%%%%%%%%%%%%%%%%%%%%%%%%%%%%%%%%%%%%%%%%%%%%%%%%%%%%%
4  function x = randnum(a,b)
5  global maxiter
6  % x will return a vector of size maxiter
7  % each component of this vector is a random
8  % number between a and b.
9  %x = a + rand(1,maxiter)*(b-a);
10 x = a + rand()*(b-a);
11 end

```


Bibliography

- [1] “Chemostat,” 2002. URL:<http://encyclopedia2.thefreedictionary.com/chemostat>. Online; accessed 24-June-2016.
- [2] H. Smith, *An Introduction to Delay Differential Equations with Applications to the Life Sciences*. 57, Springer-Verlag New York, 2011.
- [3] S. Thompson, “Delay-differential equations,” *Scholarpedia*, vol. 2, no. 3, pp. 1–42, 2007.
- [4] A. Hastings, *Encyclopedias of the Natural World : Encyclopedia of Theoretical Ecology (1)*. University of California Press, 2012.
- [5] C. Wu, H. Kim, M. Zajacc, and A. Clemm, “Sir and sirs models,” 2011. URL:https://www.gwu.edu/~spwm/Cindy_Angela_Course Online: accessed 24-June-2016.
- [6] S. Gonçalves, G. Abramson, and M. F. C. Gomes, “Oscillations in sirs model with distributed delays,” *The European Physical Journal B*, vol. 81, no. 3, pp. 363–371, 2011.
- [7] H. Bai and Y. Zhai, “Hopf bifurcation analysis for the model of the chemostat with one species of organism,” *Abstract and Applied Analysis*, vol. 2013, pp. 1–7, 2013.
- [8] X. Kang, “Chemostat,” 2000. URL:<http://userpages.umbc.edu/~xkang/ENCH772/chemostat.html> Online; accessed 24-June-2016.
- [9] W. B. Corporation, “Introduction to enzymes,” 2015. URL:<http://www.worthington-biochem.com/introbiochem/substrateconc.html>. Online; accessed 24-June-2016.
- [10] J. E. Forde, *Delay Differential Equation Models in Mathematical Biology*. PhD thesis, The University of Michigan, 2005. Ch.2, page 14-31.
- [11] S. X. H. J. W. Carrie A. Manore, Kyle S. Hickmann and J. M. Hyman, “Comparing dengue and chikungunya emergence and endemic transmission in a.aegypti and a.albopictus,” *Journal of Theoretical Biology*, vol. 356, pp. 174–191, 2014.